

Application of Phase Change Material in Buildings:

Field Data vs. EnergyPlus Simulation

by

Karthik Muruganantham

A Thesis Presented in Partial Fulfillment  
of the Requirements for the Degree  
Master of Science

Approved November 2010 by the  
Graduate Supervisory Committee:

Patrick Phelan, Chair  
Taewoo Lee  
Agami Reddy

ARIZONA STATE UNIVERSITY

December 2010

## ABSTRACT

Phase Change Material (PCM) plays an important role as a thermal energy storage device by utilizing its high storage density and latent heat property. One of the potential applications for PCM is in buildings by incorporating them in the envelope for energy conservation. During the summer season, the benefits are a decrease in overall energy consumption by the air conditioning unit and a time shift in peak load during the day. Experimental work was carried out by Arizona Public Service (APS) in collaboration with Phase Change Energy Solutions (PCES) Inc. with a new class of organic-based PCM. This “BioPCM” has non-flammable properties and can be safely used in buildings. The experimental setup showed maximum energy savings of about 30%, a maximum peak load shift of ~ 60 min, and maximum cost savings of about 30%.

Simulation was performed to validate the experimental results. EnergyPlus was chosen as it has the capability to simulate phase change material in the building envelope. The building material properties were chosen from the *ASHRAE Handbook - Fundamentals* and the HVAC system used was a window-mounted heat pump. The weather file used in the simulation was customized for the year 2008 from the National Renewable Energy Laboratory (NREL) website. All EnergyPlus inputs were ensured to match closely with the experimental parameters. The simulation results yielded comparable trends with the experimental energy consumption values, however time shifts were not observed. Several other parametric studies like varying PCM thermal conductivity, temperature range, location, insulation R-value and combination of different PCMs were analyzed and results are presented. It was found that a

PCM with a melting point from 23 to 27 °C led to maximum energy savings and greater peak load time shift duration, and is more suitable than other PCM temperature ranges for light weight building construction in Phoenix.

## ACKNOWLEDGMENTS

First of all I would like to acknowledge my advisor, Dr. Patrick Phelan for his constant encouragement and guidance throughout this research. In addition, I would also like to thank Dr. Agami Reddy for his helpful suggestions during the course of my research.

I also appreciate Mr. Peter Horwath and Mr. David Ludlam of Phase Change Energy Inc. and Mr. Timothy McDonold of Arizona Public Service for their information on the experimental testing at the APS Solar Test And Research (STAR) center. I would also like to thank Dr. Rusty Sutterlin of Entropy Solutions for providing a new set of DCS readings of the PCM for the EnergyPlus simulation.

## TABLE OF CONTENTS

	Page
LIST OF TABLES .....	vii
LIST OF FIGURES .....	ix
LIST OF SYMBOLS / NOMENCLATURE .....	xi
CHAPTER	
1 INTRODUCTION .....	1
1.1 Overview .....	1
1.2 Applications of PCM .....	2
1.3 PCM in Buildings .....	3
1.4 BioPCM Advantages and Working Principle .....	5
2 EXPERIMENTAL DATA ANALYSIS .....	7
2.1 Location .....	7
2.2 Experimental Setup .....	8
2.3 Envelope Construction .....	9
2.4 Heat Pump and Thermostat Settings .....	10
2.5 Phase Change Material (PCM) Properties .....	13
2.6 Phase Change Material (PCM) Dimensions .....	15
2.7 Actual Data and Technical Difficulties .....	17
3 SIMULATION USING ENERGYPLUS .....	18
3.1 Introduction .....	18
3.2 Comparison of Doe-2, Blast and Energyplus .....	20
3.3 Phase Change Material Capability in EnergyPlus .....	24
3.4 Objective of the Simulation .....	26

CHAPTER	Page
3.5 Weather File.....	26
3.6 PCM Thickness.....	28
3.6.1 Wall Thickness .....	28
3.6.2 Floor and Ceiling Thickness.....	30
3.7 Inputs in EnergyPlus.....	31
3.7 General Inputs in EnergyPlus.....	31
3.8 Material, Construction and Surface Detailing Inputs.....	33
3.9.1 Material Inputs.....	34
3.9.2 Construction Inputs.....	35
3.9.3 Surface Detailing.....	36
3.10 HVAC Inputs.....	37
3.10.1 Outdoor Air Mixer.....	38
3.10.2 Dx Cooling Coil.....	38
3.10.3 Dx Heating Coil.....	39
3.10.4 Fan.....	40
3.10.5 Supplemental Heater.....	41
3.10.6 Infiltration, ventilation and Thermostat inputs.....	42
3.11 Performance Curves.....	44
3.11.1 Cooling Coil.....	44
3.11.2 Heating Coil.....	45
3.12 Simulation Work Carried Out.....	47
4 RESULTS AND DISCUSSION .....	48
4.1 Overview.....	48
4.2 Thermal Resistance of the Wall with PCM and without PCM....	48

CHAPTER	Page
4.3 Experimental Results.....	50
4.3.1 Energy Consumption and Peak Load Shift.....	51
4.3.2 Cost Savings and Reduction in Energy Demand (On- peak Hours) .....	56
4.4 SIMULATION RESULTS USING ENERGYPLUS.....	61
4.4.1 Energy Consumption and Peak Load Shift.....	62
4.4.2 Variation of Thermal Conductivity of the PCM.....	64
4.4.3 Variation of the Temperature Range of the PCM.....	66
4.4.4 Variation of Location of the PCM Layer.....	70
4.4.5 Variation of Insulation Used in the Wall Cross-section.....	73
4.4.6 Variation of the PCM Temperature Range in the West and South Wall.....	75
4.4.7 Variation of the BioPCM Thickness.....	78
4.5 Virgin and Experimented PCM.....	79
5 Conclusion and Future Work .....	80
5.1 Summary and Conclusion of Present Work.....	80
5.2 Future Work.....	82
REFERENCES .....	83

## LIST OF TABLES

Table	Page
2.1 Thermostat Settings on the Shed.....	12
2.2 Properties of BioPCM.....	13
3.1 Comparison of General Features and Capabilities.....	21
3.2 Comparison of Loads Features and Capabilities.....	22
3.3 Comparison of HVAC Features and Capabilities.....	23
3.4 Enthalpy-Temperature Input.....	35
3.5 Zone Infiltration Calculation.....	43
4.1 Thermal Resistance of the Wall without PCM.....	48
4.2 Thermal Resistance of the Wall with PCM.....	49
4.3 Energy Usage and Peak Load Shift.....	51
4.4 Percentage Reduction in Peak Load.....	55
4.5 Residential Billing Cycle.....	56
4.6 Business Billing Cycle.....	57
4.7 Cost Savings by BioPCM.....	58
4.8 Cost of BioPCM in the Shed.....	58
4.9 Reduction in Energy Demand during On-Peak Hours.....	60
4.10 Energy Consumption and Peak Load Time Shift.....	62
4.11 Variation of Thermal Conductivity of the PCM.....	64
4.12 Variation of Thermal Conductivity of the PCM: Energy Savings....	65
4.13 Variation of Thermal Conductivity of the PCM: Time Shift.....	66
4.14 Variation of PCM Temperature Range: Energy Usage.....	67
4.15 Variation of PCM Temperature Range: Energy Savings.....	68
4.16 Variation of PCM Temperature Range: Time Shift.....	69



Table	Page
4.17 Variation of PCM Location: Energy Usage.....	71
4.18 Variation of PCM Location: Energy Savings and Time Shift.....	72
4.19 Variation of Insulation in the wall: Energy Usage.....	73
4.20 Variation of Insulation in the Wall: Energy Savings and Time Shift .....	74
4.21 Combination of PCM: Energy Usage.....	76
4.22 Combination of PCM: Energy Savings.....	76
4.23 Combination of PCM: Time Shift.....	77
4.24 Variation of the BioPCM Thickness.....	78

## LIST OF FIGURES

Figure		Page
1.1	Sensible and Latent Heat.....	2
1.2	Operating Principle of BioPCM.....	5
2.1	Average Daily Solar Insolation United States.....	7
2.2	Experimental Setup of South (Non BioPCM) Shed and North (with BioPCM) shed.....	8
2.3	Wall Cross-section of North Shed.....	9
2.4	AMANA Heat Pump Specifications.....	11
2.5	Heat Pump and Thermostat used in the Sheds.....	12
2.6	Specific Heat Capacity of the BioPCM.....	14
2.7	Enthalpy Profile of the BioPCM.....	15
2.8	BioPCM Mat Used in the Walls.....	16
2.9	Installed BioPCM Mat in the Ceiling.....	16
3.1	Big Picture of EnergyPlus.....	20
3.2	Single BioPCM Block Used in the Walls.....	28
3.3	Single BioPCM block used in the Ceiling and Floor.....	30
3.4	Simulation Control Class List.....	31
3.5	Schedule Compact Inputs.....	32
3.6	Zone Inputs and Global Geometry Rules.....	33
1.7	Building Material Inputs.....	34
3.8	Window Inputs.....	34
3.9	Construction Input.....	35
3.10	Building Surface Detailed.....	36

Figure	Page
3.11 Fenestration Surface Detailed.....	36
3.12 Schematic of Packaged Terminal Heat Pump.....	37
3.13 Outdoor Air Mixer Class List in EnergyPlus.....	38
3.14 DX Cooling Coil Inputs.....	39
3.15 DX Heating Coil Inputs.....	40
3.16 Fan Inputs.....	41
3.17 Electric Heater Input.....	41
4.1 Experimental Peak Curve for June (1 min).....	52
4.2 Experimental Peak Curve for July (15 min).....	53
4.3 Experimental Peak Curve for September (15 min).....	53
4.4 Experimental Peak Curve for October (15 min).....	54
4.5 Variation of Thermal Conductivity of the PCM: Energy Usage.....	65
4.6 Variation of PCM Temperature Range: Energy Savings.....	68
4.7 Variation of PCM Temperature Range: Peak Load Time Shift.....	69
4.8 Variation of PCM Location: Energy Saving.....	72
4.9 Variation of Insulation in the Wall: Energy Savings.....	74
4.10 Variation of Insulation in the Wall: Annual Energy Consumption...	75
4.11 Virgin and Experimented BioPCM.....	79

## LIST OF SYMBOLS

Symbol	Page
1. $Q_{\text{SENSIBLE}}$ - Sensible Heat .....	1
2. $\Delta Q_{\text{LATENT}}$ – Latent Heat .....	1
3. $m$ - Mass .....	1
4. $\Delta H$ – Enthalpy change.....	1
5. $\Delta h$ – Specific enthalpy change.....	1
6. $C_p$ - Specific heat capacity.....	1
7. $T$ – Temperature.....	41

## Chapter 1

### INTRODUCTION

#### 1.1 Overview

Thermal Energy Storage (TES) allows heat and cold to be stored which can be used later. It can be stored under two methods: physical methods (sensible and latent heat storage) and chemical methods. The most commonly observed thermal energy storage is by means of sensible heat. Sensible heat is the amount of heat released or absorbed by a substance during a change of temperature. It can be calculated as a product of mass, specific heat and temperature difference as

$$Q_{SENSIBLE} = m * c_p * \Delta T \quad (1.1)$$

On the other hand, latent heat is the amount of heat released or stored by a substance during a change of state that occurs without much change in temperature. Figure 1.1 shows the difference between sensible and latent heat storage. Latent heat storage can occur as solid-liquid phase change, liquid-vapor phase change, and solid-solid phase change. For solid-liquid phase change material, the latent heat stored is equal to the enthalpy difference between the solid and the liquid phase [1] and due to the small volume change, the latent heat can approximately be written as

$$\Delta Q_{LATENT} = \Delta H = m * \Delta h \quad (1.2)$$

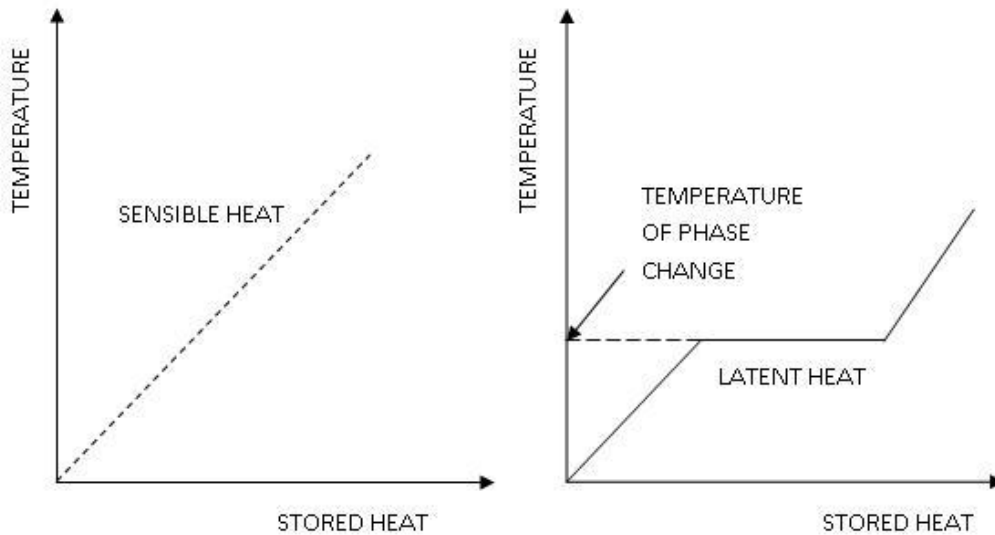


Figure 1.1 Sensible Heat and Latent Heat

The storage media employing the solid-liquid phase are commonly known as latent heat storage material or phase change material (PCM). As seen from the latent curve in Fig. 1.1, PCM can be used to store or extract heat without substantial change in temperature. Hence it can be used for temperature stabilization in an application. The main advantage of PCM is that it can store about 3 to 4 times more heat per volume than sensible heat in solids and liquids at an approximate temperature of 20 °C [1]

## 1.2 Applications of PCM

Phase Change Material (PCM) is a useful remedy when there is a mismatch between the supply and demand of energy. Some of the potential applications of PCM investigated by Salyer et al. [2] and Fatih Dermirbas [3] are shown below:

- Thermal protection of flight data and cockpit voice recorders
- Hot and cold medical therapy
- Transportation and storage of perishable foods, medicine and pharmaceuticals products
- Thermal management systems
- Solar power plants to store thermal energy during day time and reuse it during the later part of the day
- Electronic chips to prevent operation at extreme temperatures
- Photovoltaic cells and solar collectors to avoid hot spots
- Miscellaneous use like solar-activated heat pumps, waste heat recovery etc.,

One of the other potential applications of PCM is in buildings to conserve energy. This thesis focuses on the use of PCM in buildings to deliver possible energy savings and peak load time shift. By offsetting the occurrence of peak load, few power plants can be operated to meet the load requirements. This saves initial cost, operating cost of the power plants and reduces harmful emissions.

### 1.3 PCM in Buildings

The global demand for air conditioning has increased significantly in the past decade and huge demands in electric power consumption have led to increased interest in energy efficiency and conservation, as studied by Dincer and Rosen [4]. Energy consumption in buildings varies significantly during the day and night according to the demand by business and residential activities. In

hot climate areas, most of the energy is consumed during the day time due to high ambient temperatures and intense solar radiation. This has led to varying pricing system for the on-peak and off-peak periods of energy use. Potential cost savings by reduction in energy consumption and by shift of peak load during the day can be achieved by incorporating PCMs in the envelope of residential and business building establishments.

There are several promising ongoing developments in the field of PCM applications for heating and cooling of buildings. Frank [5] reviewed using PCM in the walls and in the ducts of the cooling units of a building to provide both heating and cooling effects. Pasupathy et al. [6] performed experimental and simulation analysis of incorporating PCM in the roofs of buildings. Guo [7] carried out an experimental work on a new kind of PCM and found that its heat storing/releasing ability was significantly higher than other PCMs. He also performed a simulation and calculation based on the effective heat capacity method to verify the results. Huang [8] applied a validated model to predict the energy conserving capability of the PCM by fabricating them in walls of buildings. An experimental study was conducted by Takeda et al. [9] to analyse PCM usage on floor supply air conditioning systems to enhance building thermal mass. Similar work by Farid and Chen [10] presented a simulation of under-floor heating with and without the presence of a PCM layer. Frank [11] studied a storage system for both heating and cooling seasons that comprised two different PCMs integrated into a reverse cycle refrigeration heat pump system.



#### 1.4 BioPCM Advantages and Working Principle

Many PCMs are derived from paraffin-based materials which are highly flammable and thus hinders their use in buildings. A newly developed organic-based PCM, here termed 'BioPCM' improves safety since it is less flammable than traditional PCMs. Fire retardant materials can also be added to paraffin-based PCMs to reduce their flammability, but at the expense of altering the thermophysical properties of the material. The BioPCM can also be manufactured such that the melting point can be varied between  $-22.7\text{ }^{\circ}\text{C}$  to  $78.33\text{ }^{\circ}\text{C}$  ( $-73\text{ }^{\circ}\text{F}$  to  $+173\text{ }^{\circ}\text{F}$ ), and this facilitates its use in various climatic zones.

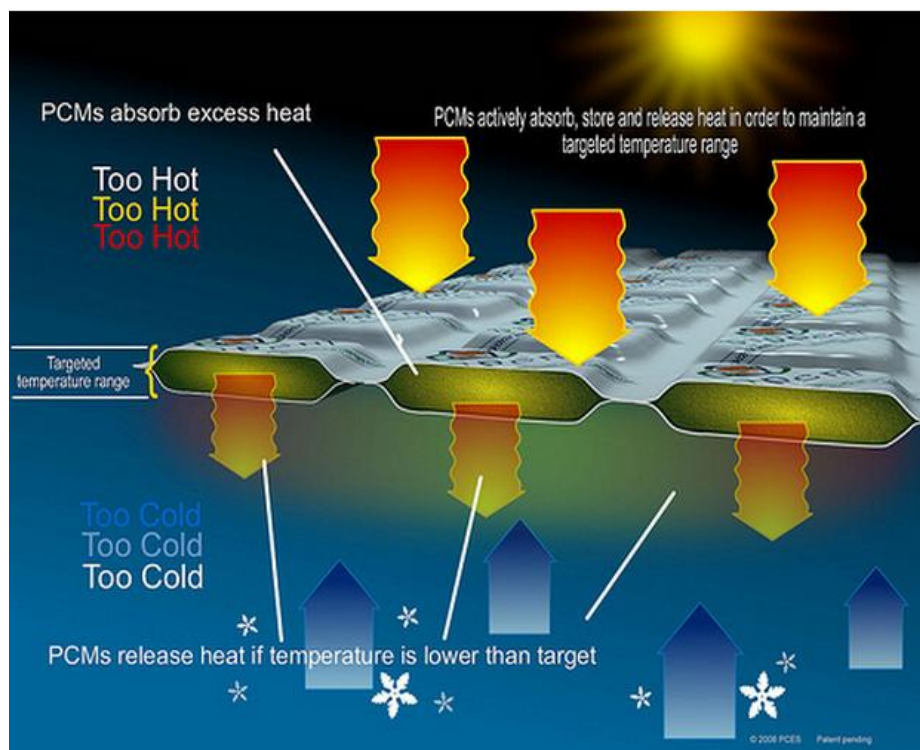


Figure 1.2 Operating Principle of BioPCM

(Source: phasechangeenergy.com)

As seen in Fig. 1.2, BioPCM are encapsulated as discrete blocks with air gaps between them. These mats are placed in the building envelope (walls, floor and ceiling). During the day time with high ambient temperature and solar radiation, the BioPCM melts (changes phase from solid to liquid) storing large amounts of thermal energy. This is called the melting or charging process. During this process heat gain into the building is reduced, and hence less energy is consumed by the HVAC system to cool the building. During the night time, the PCM changes phase from liquid back to solid phase dissipating heat both into the building and to the outside environment. This process is called solidification or discharging process. This process is advantageous during the winter time as the released heat aids in warming the building. However, it has drawbacks during the summer season as the extra heat discharged has to be removed by the HVAC system.

## Chapter 2

### EXPERIMENTAL DATA ANALYSIS

#### 2.1 Location

The experimental work was carried out at the Arizona Public Service (APS) Solar Testing and Research (STAR) center in Tempe, Arizona (in the Phoenix metropolitan area). The primary reason for choosing Arizona as the testing location is because of its abundant availability of solar insolation, dry weather and very little precipitation during the year. Figure 2.1 below shows the average daily solar insolation available in the United States with Arizona receiving an average of 6000 to 6500 Watt/hours per square meter per day [17].

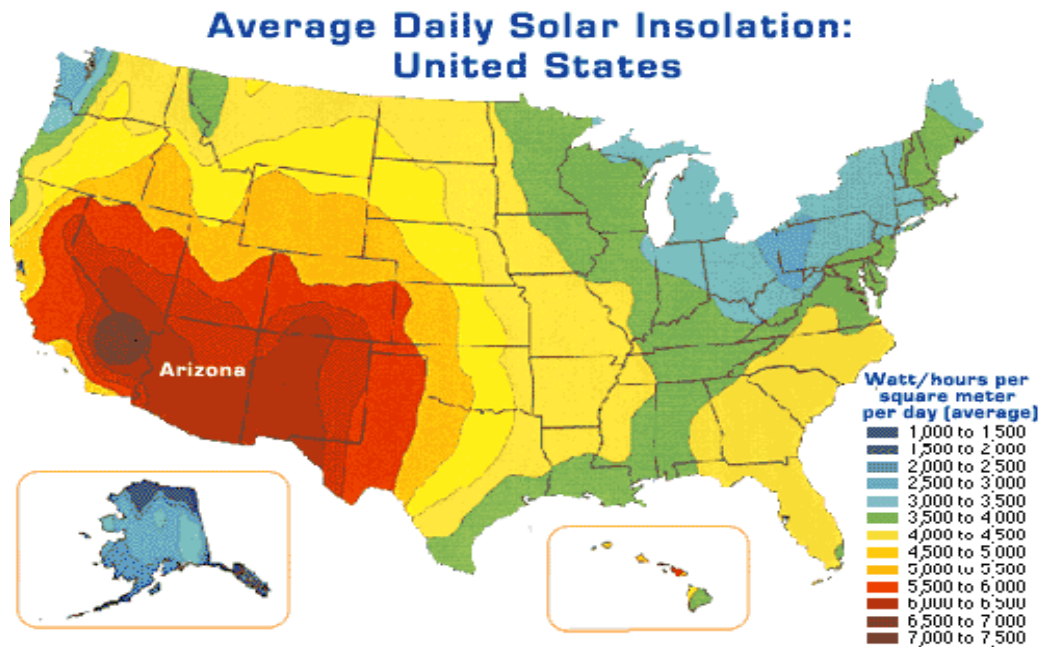


Figure 2.1 Average Daily Solar Insolation

(Source: [www.solidsolar.com](http://www.solidsolar.com))

From Fig 2.1, it can be inferred that the south western part of the United States will consume more electric energy (cooling loads) to maintain residential and commercial buildings at comfort level during the summer months. Hence PCM with its high thermal energy storage and peak load offset capability can potentially save huge electric power consumption in these regions.

## 2.2 Experimental Setup

The experimental setup was designed and testing was carried out by APS and Phase Change Energy Inc. at the STAR facility. Arizona State University entered the project after completion of the testing and only analyzed the experimental data. The data were collected for the entire 2008 calendar year. The set up consists of two nominally identical sheds as shown in Fig 2.2, named as the 'North' and 'South' sheds with length, width and height as 4.876 m x 3.657 m x 2.43 6m (16' x 12' x 8') and with a 4/12 pitch roof.



Figure 2.2 Experimental Setup of South (non BioPCM) Shed and North (BioPCM) shed

Both sheds face east and were located to ensure that there were no shading and had unobstructed wind flows. The two sheds were fitted with identical heat pumps and connected to separate three-phase electricity meters in order to monitor the electric consumption by the HVAC system.

### 2.3 Envelope Construction

The north shed had BioPCM mat layer in all the four walls, ceiling and floor with different thicknesses, whereas the south shed was of conventional construction without any installed BioPCM. Walls were constructed with 2" x 4" studs 16" O.C. with R-13 fiberglass insulation, T-111 siding and 1/2" finished gypsum board. The wall cross-section of the North shed is shown in Fig 2.3.

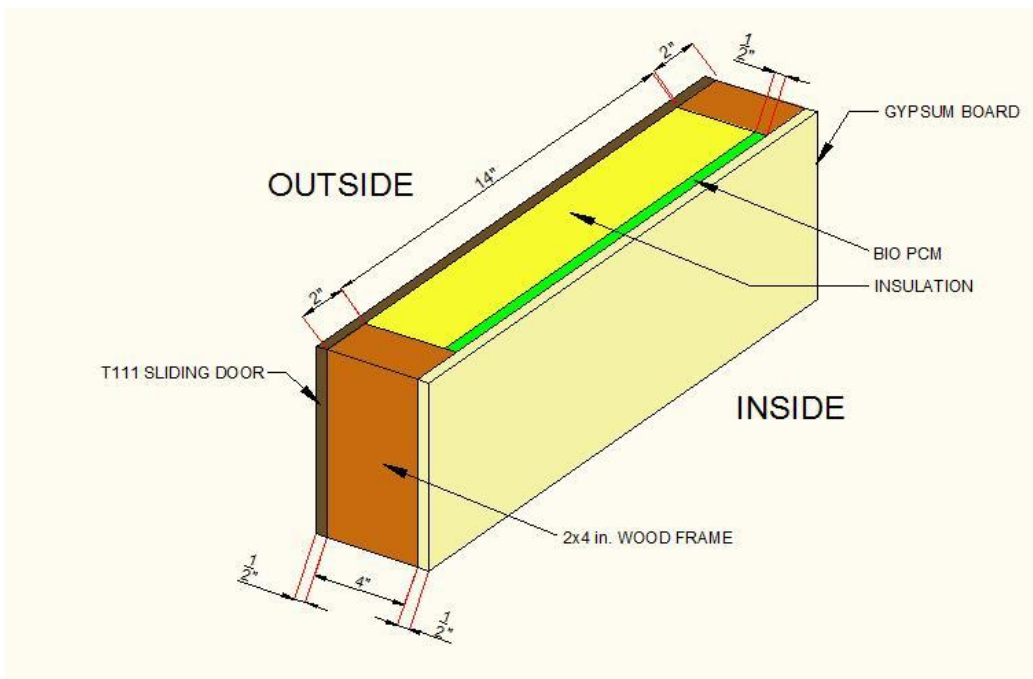


Figure 2.3 Wall Cross-section of the North Shed

The structures had enclosed attic space with R-19 fiberglass batt insulation between 24" O.C. of ceiling. 1/2" OSB roof sheathing was covered with

15 lb. roofing felt and standard three tab fiberglass desert tan shingles. Standard BioPCM mat with a PCM density of 0.56 lbs. per cubic foot was installed in all walls between the fiberglass insulation and gypsum board of the north shed. In addition, 1 lb. per cubic foot density BioPCM was installed in both the ceiling and floor of the North shed.

Each shed had two standard louvered rectangular vents on the attic of the south and north walls. In addition a wooden door and a single-pane glass window were located on the east side of both the sheds. The dimensions of the door were 6.5' x 2.5' (height x width) and that of the window was 1.6' x 2.5' (height x width).

#### 2.4 Heat Pump and Thermostat Settings

Both sheds were fitted with identical Amana AH093A35MA window-mounted heat pumps to study the energy consumption and to establish the performance of the BioPCM. The specifications of the heat pump are shown in Fig 2.4. Two Honeywell 7500 series 7-day programmable thermostats replaced the conventional thermostats on May 30<sup>th</sup> 2008 to yield accurate results. They were selected after bench testing where they were shown to have less than 0.1 °F variation between the two. An interface relay panel was installed for each building. Figure 2.5 shows the heat pump and programmable thermostats used in the sheds.


<b>Amana Models</b>		<b>AH093A35MA</b>
		
<b>General Features:</b>		
Voltage		230/208
Discharge Air		Top
Auto Air Swing		No
Slide-out Filter		Side Pull-out
Approx. Chassis Wgt.		98 lbs
Approx. Shipping Wgt.		114 lbs
<b>Cooling:</b>		
Capacity / BTUH		9,300 / 9,100
Amps		4.6 / 4.8
Watts		990 / 970
CFM		310
E.E.R.		10.0 / 10.0
Dehumidification - pts/hr		2.2
<b>Electric Heat:</b>		
Capacity / BTUH		10,700 / 8,500
Amps		14.8 / 13.4
Watts		3,416 / 2,792
<b>Heat Pump: (Reverse cycle)</b>		
Capacity / BTUH		8,400 / 8,100
Amps		4.0 / 4.2
Watts		920 / 900
C.O.P		2.8 / 2.8
Adjustable Change-Over Thermostat		Yes
Thermostatic Drain Valve		Yes

Figure 2.4 AMANA Heat Pump Specifications

(Source: <http://www.amana-ptac.com>)



Figure 2.5 Heat Pump and Thermostats used in the Shed

After the installation of the programmable thermostats, the thermostat settings were set to auto switchover mode for all the 7 days. The thermostat settings are shown in Table 2.1.

Table 2.1 Thermostat Settings on the Sheds

TIME (Hours)	HEAT °C (°F)	COLD °C (°F)
6:00	22.7 (73)	25.0 (77)
8:00	22.7 (73)	25.0 (77)
18:00	22.7 (73)	25.0 (77)
20:00	20.5 (69)	22.3 (72)



## 2.5 Phase Change Material (BioPCM) Properties

The properties of the BioPCM used in the experimental setup are described in Table 2.2. Additionally, a commonly available paraffin-based PCM, GR27 researched by Huang [7] and water properties are shown for comparison.

Table 2.2 Properties of BioPCM

Description	BioPCM	GR27	Water
Melting Point (°C)	29	28	0
Density (kg/m <sup>3</sup> )	860	710	1000
Specific Heat (kJ kg <sup>-1</sup> °C <sup>-1</sup> )	1.97	1.125	4.179
Latent Heat (kJ/kg)	219	72	334
Viscosity @ 30 °C (cp)	7	-	0.798
Boiling Point (°C)	418	-	100
Thermal Conductivity (W m <sup>-1</sup> °C <sup>-1</sup> )	0.2	0.15	0.6

The phase change temperature range for the BioPCM was from 27 to 31 °C. The value of 29 °C was chosen to conventionally represent the approximate peak of the heating curve. The BioPCM offers significant advantage over the conventional PCM with its high specific heat and high latent capacity. On the other hand, water with its superior properties could be an ideal candidate for PCM applications in buildings. However, it cannot be used in buildings because of storage-associated problems and as the liquid-gas phase change occurs at a higher temperature (boiling point) which is not possible to reach in ordinary situations.

The heat capacity and temperature profile values were obtained using a Differential Scanning Calorimeter (DSC). A PCM sample of 2.73 mg was tested

by Dr. Rusty Sutterlin of Entropy Solutions using a TA Instruments Q2000 series differential scanning calorimeter. The enthalpy values were obtained using the equations.

$$\Delta H = C_p * \Delta T \quad (2.1)$$

$$H, new = H, old + \{C_p * (T, new - T, old)\} \quad (2.2)$$

The specific heat capacity and the enthalpy profile of the BioPCM are shown in Figs 2.6 and 2.7. From the heat capacity curve, it can be inferred that the solid to liquid transition occurs at the phase change temperature range of 27 to 31 °C. From the enthalpy curve it is evident that the enthalpy at liquid phase is higher than the solid phase.

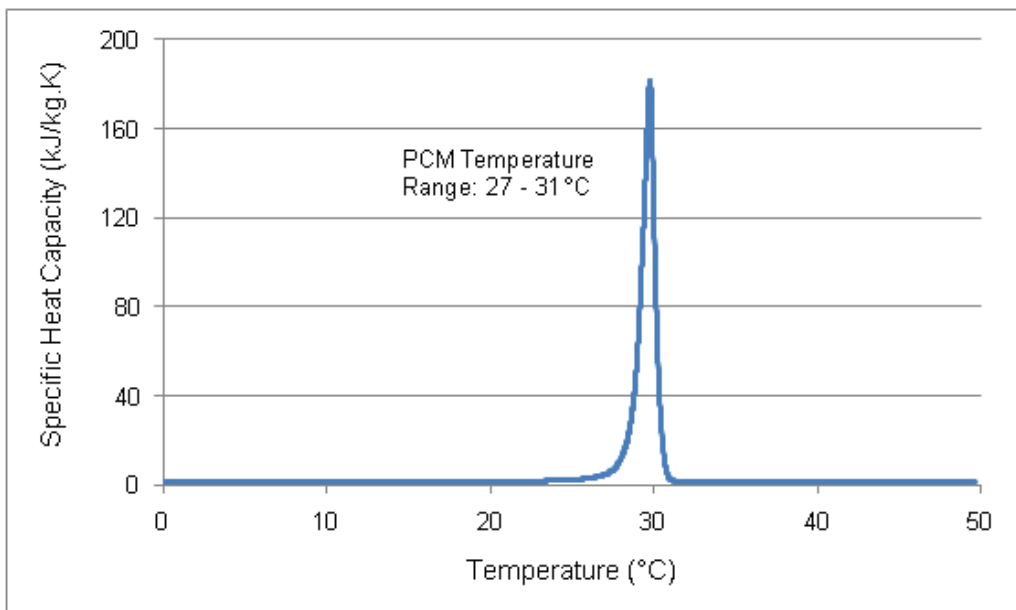


Figure 2.6 Specific Heat Capacity of the BioPCM

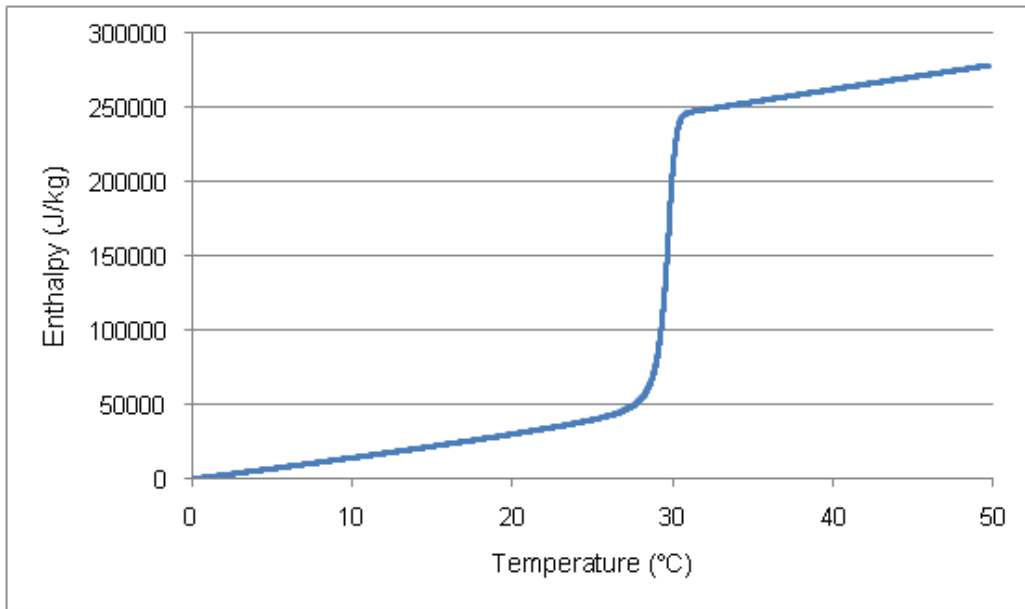


Figure 2.7 Enthalpy Profile of the BioPCM

## 2.6 Phase Change Material (BioPCM) Dimensions

The BioPCM is not packaged as a continuous sheet, but rather is organized into small blocks that are separated from one another as pictured in Fig 2.8. The BioPCM mat in the walls has 60 square blocks per 24" x 16" size of mat, with each block of dimension 1.3" x 1.3". For attic space, a BioPCM mat consisted of 4 rectangular blocks per 24" x 16" size of mat, with each individual block of dimension 7" x 11". The installed BioPCM mat in the ceiling is shown in Fig 2.9.



Figure 2.8 BioPCM Mat used in the Walls



Figure 2.9 Installed BioPCM Mat in the Ceiling

In general, volumetric expansion of the liquid phase is expected to be around 10% [1]. Hence, during manufacturing suitable precautions are taken for volumetric expansion of BioPCM during phase change and to prevent rupturing of the encapsulation.

## 2.7 Actual Data and Technical Difficulties

The data recorded at the experimental site were ambient temperature, power consumption and energy usage. In addition several thermocouples were placed at different locations in the sheds and temperatures were recorded.

The following were the technical difficulties faced during the experiment.

- The door of the shed had blown open and was replaced in January 2008.
- 50% of the wall BioPCM was replaced with identical density BioPCM on June 21<sup>st</sup> 2008 due to film issues.
- Two attic vents were installed in each shed on June 21<sup>st</sup> 2008
- Programmable thermostats were installed on May 30<sup>th</sup> 2008.
- The experimental data were initially recorded every 10 min for the month of January, February, March and December, and every 1 min for the remaining months.
- The actual data were available for 291 out of 366 days.

## Chapter 3

### SIMULATION USING ENERGYPLUS

#### 3.1 Introduction

EnergyPlus is a building energy simulation program offered by the United States Department of Energy (DOE). It can be downloaded free of cost from <http://apps1.eere.energy.gov/buildings/energyplus/>. It provides engineers, architects, and researchers the tools to model heating, cooling, lighting, ventilation, energy flows, and water use. By modeling the performance of a building, the software enables building users to optimize the building design to use less energy and water.

EnergyPlus has its origins from two existing programs: BLAST and DOE-2. BLAST (Building Loads Analysis and System Thermodynamics) and DOE-2 were both energy and load simulation tools that were developed in the late 1970s and early 1980s. EnergyPlus, like its predecessor is an energy analysis and thermal load simulation program. It requires the user to input various parameters like construction and materials details of the buildings, HVAC systems, schedules etc., to calculate the heating and cooling loads to maintain the building at the required setpoint. It also have provisions to size the system, plant equipment or zone based on the user requirements and can perform many other analysis that are necessary to verify that the simulation is performing as the actual building would.

In addition to modeling energy flows and water use, EnergyPlus includes many innovative simulation capabilities: time-steps less than an hour, modular systems and plant integrated with heat balance-based zone simulation, multi-zone air flow, thermal comfort, water use, natural ventilation, photovoltaic

systems, atmospheric pollution calculation, solar collector module, turbine module etc.

However, Energyplus has some setbacks:

1. It is not a user interface program, but there are several third-party developed interfaces that can be wrapped around EnergyPlus. Examples include design builder, OpenStudio plug-in etc.
2. It is not a life cycle cost analysis tool. (EnergyPlus version 6.0.0 released on Oct 18<sup>th</sup> 2010 overcomes this drawback)
3. It works on “garbage in, garbage out” standard. It doesn’t check for input, except for a very limited number of basic checks.

The structural improvements of EnergyPlus over BLAST and DOE-2 facilitate the code to be much more object-oriented and modular in nature. The advantage of modularity is that researchers around the world can develop their own modules with only a limited knowledge of the entire program structure.

Figure 3.1 below shows the overall program structure, links to various other programs and capability to add future modules. EnergyPlus has three basic requirements – a simulation manager, a heat and mass balance module, and a building systems simulation module. The simulation manager controls the entire simulation process. The heat balance calculations are based on IBLAST – a research version of BLAST with integrated HVAC systems and building loads simulation.

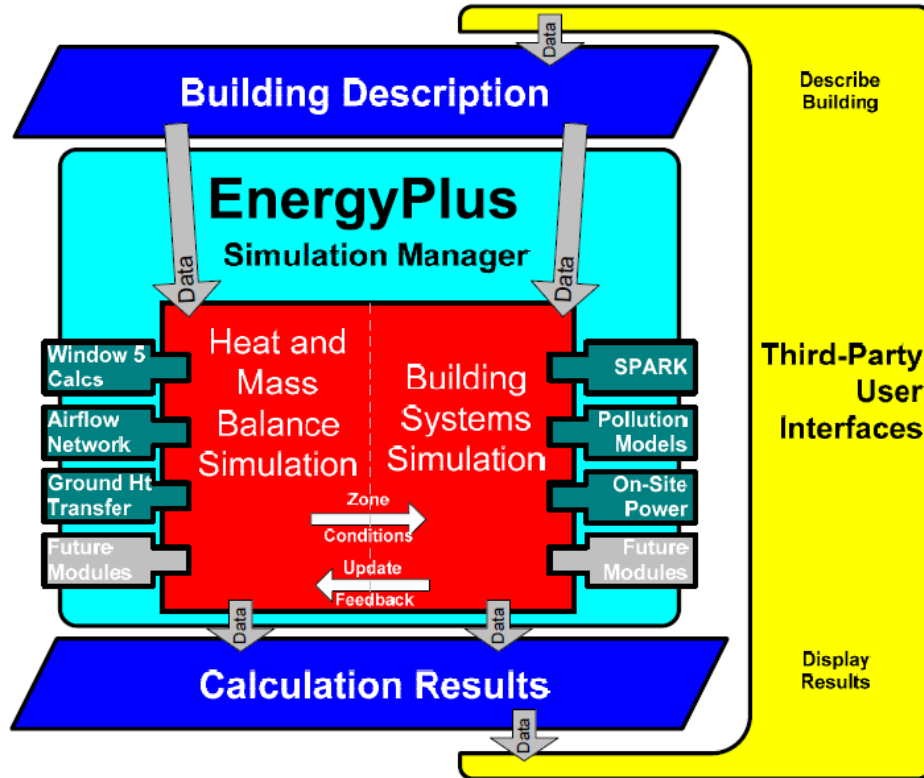


Figure 3.1 Big Picture of EnergyPlus

(Source: EnergyPlus Documentation)

### 3.2 Comparison of Doe-2, Blast and Energyplus

A comparison of major features and capabilities of DOE-2, BLAST and EnergyPlus are shown in Tables 3.1, 3.2 and 3.3. Table 3.1 shows general features, Table 3.2 load calculation features and Table 3.3 HVAC features.



Table 3.1 Comparison of General Features and Capabilities

General Feature	DOE-2	BLAST	EnergyPlus
<b>Integrated, Simultaneous Solution</b>			
• Integrated loads/system/plant	No	No	Yes
• Iterative solution	No	No	Yes
• Tight coupling	No	No	Yes
<b>Multiple Time Step Approach</b>			
• User-defined time step	No	No	Yes
• Variable time step	No	No	Yes
<b>Input Functions</b>			
• User can modify code without recompiling	Yes	No	Yes
<b>Reporting Mechanism</b>			
• Standard reports	Yes	Yes	Yes
• User-defined reports	Yes	No	Yes
• Visual surface input	No	No	Yes

Source: Strand, Richard et al. 2000

Table 3.2 Comparison of Loads Features and Capabilities

Loads feature	DOE-2	BLAST	EnergyPlus
<b>Heat balance calculation</b>			
<ul style="list-style-type: none"> <li>• Simultaneous calculation of radiation and convection processes</li> </ul>	No	Yes	Yes
<b>Interior surface convection</b>			
<ul style="list-style-type: none"> <li>• Dependent on temperature and air flow</li> </ul>	No	Yes	Yes
<ul style="list-style-type: none"> <li>• Internal thermal mass</li> </ul>	Yes	Yes	Yes
<b>Moisture absorption/desorption</b>			
<ul style="list-style-type: none"> <li>• Combined heat and mass transfer in building envelopes</li> </ul>	No	No	Yes
<b>Thermal comfort</b>			
<ul style="list-style-type: none"> <li>• Human comfort model</li> </ul>	No	Yes	Yes
<b>Anisotropic sky model</b>			
<ul style="list-style-type: none"> <li>• Sky radiance depends on sun position</li> </ul>	Yes	No	Yes
<b>Advanced fenestration calculations</b>			
<ul style="list-style-type: none"> <li>• Controllable window blinds</li> </ul>	Yes	No	Yes
<ul style="list-style-type: none"> <li>• Electrochromic glazing</li> </ul>	Yes	No	Yes
<b>WINDOW 5 calculations</b>			
<ul style="list-style-type: none"> <li>• More than 200 window types</li> </ul>	Yes	No	Yes
<ul style="list-style-type: none"> <li>• Layer-by-layer input for glazing</li> </ul>	No	No	Yes
<b>Daylighting illumination and controls</b>			
<ul style="list-style-type: none"> <li>• Interior illuminance from windows and skylights</li> </ul>	Yes	No	Yes
<ul style="list-style-type: none"> <li>• Step, dimming, luminaire controls</li> </ul>	Yes	No	Yes
<ul style="list-style-type: none"> <li>• Glare simulation and control</li> </ul>	Yes	No	Yes
<ul style="list-style-type: none"> <li>• Effects of dimming</li> </ul>	Yes	No	Yes

Table 3.3 Comparison of HVAC Features and Capabilities

HVAC systems and equipment feature	DOE-2	BLAST	EnergyPlus
<b>Fluid loops</b>			
• Connect primary equipment and coils	No	No	Yes
• Hot water loops, chilled water & condenser loops, refrigerant loops	No	No	Yes
<b>Air loops</b>			
• Connect fans, coils, mixing boxes, zones	No	No	Yes
User-configurable HVAC systems	No	No	Yes
<b>High-temperature radiant heating</b>			
• Gas/electric heaters, wall radiators	No	Yes	Yes
<b>Low-temperature radiant heating/cooling</b>			
• Heated floor/ceiling	No	No	Yes
• Cooled ceiling	No	No	Yes
<b>Atmospheric pollution calculation</b>			
• CO <sub>2</sub> , SO <sub>x</sub> , NO <sub>x</sub> , CO, particulate matter and hydrocarbon production	Yes	Yes	Yes
• On-site and at power plant	Yes	Yes	Yes
• Calculate reductions in GHG	Yes	Yes	Yes
SPARK link	No	No	Yes
TRNSYS link	No	No	Yes

Source: Strand, Richard et al. 2000

### 3.3 Phase Change Material Capability in Energyplus

In energyplus, the surface constructions in a thermal zone are simulated as one dimensional heat transfer paths through the various layers. The conventional way of simulating the heat transfer is by Conduction Transfer Functions (CTF) which describes transient conduction process with time series coefficients in an algebraic equation. The fundamental form of conduction transfer function for inside flux and outside flux are respectively:

$$q_{ki}''(t) = -Z_o T_{i,t} - \sum_{j=1}^{nz} Z_j T_{i,t-j\delta} + Y_o T_{o,t} + \sum_{j=1}^{nz} Y_j T_{o,t-j\delta} + \sum_{j=1}^{nq} \varphi_j q_{ki,t-j\delta}'' \quad (3.1)$$

$$q_{ko}''(t) = -Y_o T_{i,t} - \sum_{j=1}^{nz} Y_j T_{i,t-j\delta} + X_o T_{o,t} + \sum_{j=1}^{nz} X_j T_{o,t-j\delta} + \sum_{j=1}^{nq} \varphi_j q_{ko,t-j\delta}'' \quad (3.2)$$

In the above equations, the subscript following the comma indicates the time period. The first term in the above series (with subscript 0) has been separated from the rest to enable solving the current temperature in the solution scheme. State space method is used in EnergyPlus to determine CTF coefficients.

The advantage of Conduction Transfer Function is that with unique, simple linear equations with constant coefficients, the conduction heat transfer through a complete layer in a construction surface can be calculated. However, the constant property serves as a demerit for the CTF as it not possible to simulate temperature dependent thermal properties (variable thermal conductivity or phase change material). And it not feasible to find the temperature profile within the wall.

EnergyPlus models phase change material and variable thermal conductivity using implicit finite difference scheme coupled with enthalpy-temperature function.

$$\frac{\rho C_p \Delta x (T_{i,new} - T_{i,old})}{\Delta t} = \frac{k(T_{i-1,new} - T_{i,new})}{\Delta x} + \frac{k(T_{i+1,new} - T_{i,new})}{\Delta x} \quad (3.3)$$

The above equation shows the implicit formulation for an internal node. The subscript refers to the node and time step. The equation is supplemented with an enthalpy- temperature function:

$$h_i = f_{ht}(T_i) \quad (3.4)$$

where the function  $f_{ht}$  is supplied as an input by the user. The above two equations are used for all nodes (external surface nodes, internal surface nodes, internal nodes and nodes at material interfaces). The material interface node facilitates the use of phase change material. Since the solution is implicit, a Gauss-Seidell iteration scheme is used to update new node temperature in the construction layer. As a result, for every iteration, the node enthalpy gets updated and is used to develop a variable  $C_p$  using an additional equation.

$$C_p = \frac{h_{i,new} - h_{i,old}}{T_{i,new} - T_{i,old}} \quad (3.5)$$

This iteration scheme ensures the use of correct enthalpy and hence the respective  $C_p$  in each time step. If the material is irregular, the constant  $C_p$  provided by the user is used in the simulation.

### 3.4 Objective of the Simulation

EnergyPlus was primarily chosen for the simulation because of its capability in handling material property like phase change and variable thermal conductivity as discussed in the previous section. The main objective of the simulation is to validate energy savings and observe time shift in peak load using phase change material (PCM) in the building envelope. Secondary goals are maximize building performance by varying PCM thermal conductivity, temperature range, location, R-value and using combination of PCM in the building envelope. The penultimate version 5.0.0 was used for the simulation which was available late April 2010.

### 3.5 Weather File

The experimental testing was carried out for the calendar year 2008. The TMY3 (Typical Meteorological Year 3) weather data for Phoenix location in EPW (EnergyPlus Weather File) format was obtained from <http://www.eere.energy.gov/>. In order to compare the experimental and simulation results more accurately, the weather file was modified with actual data for the year 2008 from National Renewable Energy Laboratory (NREL) weather source. The EnergyPlus weather file requires the following inputs: dry bulb temperature ( $^{\circ}\text{C}$ ), dew point temperature ( $^{\circ}\text{C}$ ), relative humidity (%), atmospheric pressure ( $\text{Pa}$ ), extra-terrestrial horizontal and direct normal radiation ( $\text{Wh}/\text{m}^2$ ), horizontal infrared radiation intensity from sky ( $\text{Wh}/\text{m}^2$ ), global horizontal and diffuse horizontal radiation ( $\text{Wh}/\text{m}^2$ ), direct normal radiation ( $\text{Wh}/\text{m}^2$ ), global

horizontal and diffuse horizontal illuminance (*lux*), direct normal illuminance (*lux*), zenith Luminance (*Cd/m<sup>2</sup>*), wind direction (*deg*), wind speed (*m/s*), total sky cover (*0.1*), opaque sky cover (*0.1*), visibility (*km*), precipitable water (*mm*), aerosol optical depth (*0.001*), snow depth (*cm*), days since last snow, albedo (*0.01*), liquid precipitation depth (*mm*) and liquid precipitation quantity (*hour*).

The dew point was calculated using dry bulb temperature and relative humidity as follows:

$$B = \frac{\ln\left(\frac{RH}{100}\right) + \frac{(17.27 \cdot T)}{(237.3 + T)}}{17.27} \quad (3.6)$$

$$D = \frac{237.3 \cdot B}{1 - B} \quad (3.7)$$

where:

T = Dry bulb temperature (°C)

R<sub>H</sub> = Relative Humidity (%)

B = intermediate value (no units)

D = Dew point temperature (°C)

The first seven of the above inputs were taken from NREL and the remaining values used for the customized weather file are the default values used in the TMY3. The EPW weather file was initially converted into Comma Separated Value (CSV) using the EnergyPlus inbuilt weather converter. Then actual data was modified for the year 2008 and the file was reconverted back to EPW format.

### 3.6 PCM Thickness Calculation

The BioPCM used in the experimental setup is in the form of a mat consisting of PCM in plastic encapsulations hereby termed as blocks. Square blocks are used for the walls and rectangular blocks for the floor and ceiling. The blocks in the walls differ in thickness with the blocks in floor/ceiling. However, all blocks are separate from each other with air-gap between them.

The PCM module in EnergyPlus allows creation of the PCM material as a continuous layer rather than blocks. In order to ensure that the same volume of PCM tested in the experiment is also used for simulation, the thickness of the PCM layer was calculated and taken as input for EnergyPlus.

#### 3.6.1 Wall Thickness

The BioPCM mat located in the walls contains 60 square blocks per 24" x 16" (0.609 m x 0.406 m) size of mat, with each block having dimension 1.3" x 1.3" (0.033 m x 0.033 m) and thickness 0.3" (0.0076 m). The dimension of a single PCM block used in the walls is shown in Fig 3.2

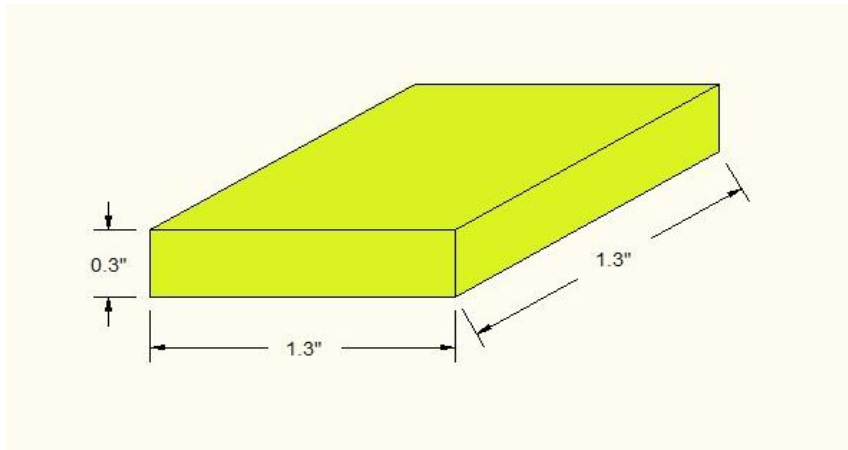


Figure 3.2 Single BioPCM Block Used in the Walls



$$\begin{aligned}\text{The volume of PCM in a block} &= 0.033 \text{ m} \times 0.033 \text{ m} \times 0.0076 \text{ m} \\ &= 8.308 \times 10^{-6} \text{ m}^3\end{aligned}$$

$$\begin{aligned}24'' \times 16'' \text{ of BioPCM mat with 60 blocks (0.0654 m}^2\text{) contains} \\ &= 60 \times 8.308 \times 10^{-6} \text{ m}^3 \\ &= 5 \times 10^{-4} \text{ m}^3 \text{ of PCM}\end{aligned}$$

Therefore, 24'' x 16'' (0.247 m<sup>2</sup>) of BioPCM mat as a continuous layer will contain  $5 \times 10^{-4} \text{ m}^3$  of PCM with thickness,  $T_{\text{PCM,WALL}} = \mathbf{0.00202 \text{ m}}$

### 3.6.2 Floor and Ceiling Thickness

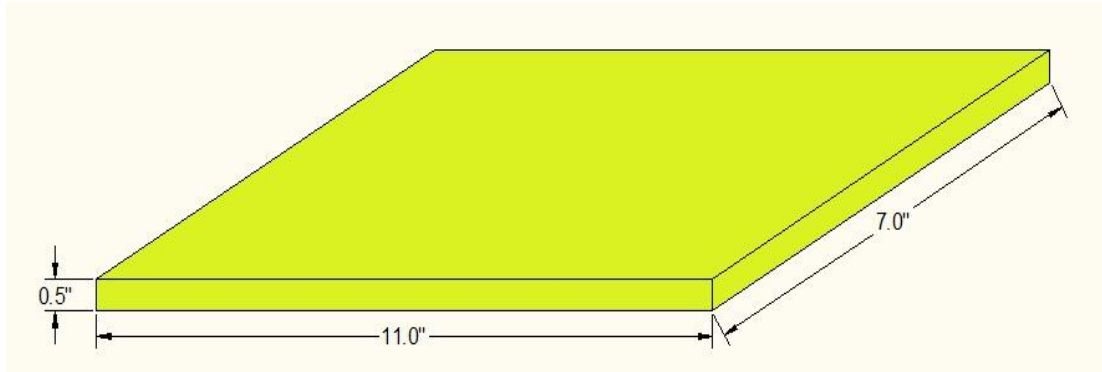


Figure 3.3 Single BioPCM block used in the Ceiling and Floor

Similarly, the BioPCM mat in the floor and ceiling has 4 rectangular blocks per 24" x 16" (0.609 m x 0.406 m) size of mat, with each block of dimension 11" x 7" (0.279 m x 0.178 m) and with thickness 0.5" (0.0127 m).

$$\begin{aligned}\text{The volume of PCM in a block} &= 0.279 \text{ m} \times 0.178 \text{ m} \times 0.0127 \text{ m} \\ &= 6.307 \times 10^{-4} \text{ m}^3\end{aligned}$$

$$\begin{aligned}24" \times 16" \text{ of bioPCM mat with 4 blocks (0.198 m}^2\text{) contains} \\ &= 4 \times 6.307 \times 10^{-4} \text{ m}^3 \\ &= 2.52 \times 10^{-3} \text{ m}^3 \text{ of PCM}\end{aligned}$$

Therefore, 24" x 16" (0.247 m<sup>2</sup>) of BioPCM mat as a continuous layer will contain 2.52 x 10<sup>-3</sup> m<sup>3</sup> of PCM with thickness:

$$\mathbf{T_{PCM, CEILING} = 0.0102 \text{ m} \text{ and } T_{PCM, FLOOR} = 0.0102 \text{ m}}$$

### 3.7 Inputs in Energyplus

The EnergyPlus inputs have been divided into the following categories:

1. General inputs
2. Material and construction inputs
3. HVAC inputs

These inputs are described in detail in the subsequent sections. Screen shots of EnergyPlus have been provided for some of the important inputs.

### 3.8 General Inputs in Energyplus

Some of the general inputs used in EnergyPlus are described below:

- Version

The version input describes the EnergyPlus version and the value was taken as 5.0.0

- Simulation Control

The simulation control field describes the calculations that are required to be performed by EnergyPlus. Fig 3.4 shows simulation control class list.

Field	Units	Obj1
Do Zone Sizing Calculation		No
Do System Sizing Calculation		No
Do Plant Sizing Calculation		No
Run Simulation for Sizing Periods		No
Run Simulation for Weather File Run Periods		Yes

Figure 3.4 Simulation Control Class List

- Building

The important buildings inputs required loads convergence tolerance value (default value of 0.04 was taken), temperature convergence tolerance

value (default value of 0.4 was taken) and maximum number of warmup days (default value of 25 was taken).

- Surface Convection Algorithm: Inside and Outside

Detailed Algorithm was selected for both the inside and outside cases. The detailed natural convection model correlates the heat transfer coefficient to the temperature difference for various orientations.

- Heat Balance Algorithm and Timestep

The heat balance algorithm used for both the PCM and the non PCM shed was conduction finite difference. It was selected because of its capability to handle phase change material. The timestep value of 20 per hour was chosen as suggested for the conduction finite difference algorithm.

- Schedule

Schedule compact (Fig 3.5) was chosen for its simplicity. The following are the inputs.

Field	Units	Obj1	Obj2	Obj3	Obj4	Obj5	Obj6	Obj7	Obj8
Name		Heating or Cooling	CoolingCoilAvalSch hed	HeatingCoilAvalSch hed	CyclingFanSch	INFIL-SCH	FanAndCoilAvalSch hed	Heating Setpoints	Cooling Setpoints
Schedule Type Limits Name		Control Type	Fraction	Fraction	Fraction	Fraction	Fraction	Temperature	Temperature
Field 1	varies	Through: 12/31	Through: 12/31	Through: 12/31	Through: 12/31	Through: 12/31	Through: 12/31	Through: 12/31	Through: 12/31
Field 2	varies	For: AllDays	For: AllDays	For: AllDays	For: AllDays	For: AllDays	For: AllDays	For: AllDays	For: AllDays
Field 3	varies	Unit: 24.00	Unit: 24.00	Unit: 24.00	Unit: 24.00	Unit: 24.00	Unit: 24.00	Unit: 6.00	Unit: 6.00
Field 4	varies	4	1	1	0	1	1	20.5	22.3
Field 5	varies							Unit: 8.00	Unit: 8.00
Field 6	varies							22.7	25
Field 7	varies							Unit: 20.00	Unit: 20.00
Field 8	varies							22.7	25
Field 9	varies							Unit: 24.00	Unit: 24.00
Field 10	varies							20.5	22.3
Field 11	varies								

Figure 3.5 Schedule Compact Inputs

- Zone and Global Geometry Rules

The zone and global geometry rule inputs are shown in the Fig 3.6 below.

Field	Units	Obj1	Obj2
Name		Attic	LIVING ZONE
Direction of Relative North	deg	0	0
X Origin	m	0	0
Y Origin	m	0	0
Z Origin	m	0	0
Type		1	1
Multiplier		1	1
Ceiling Height	m	autocalculate	autocalculate
Volume	m <sup>3</sup>	autocalculate	autocalculate
Zone Inside Convection Algorithm			
Zone Outside Convection Algorithm			
Part of Total Floor Area			

Field	Units	Obj1
Starting Vertex Position		UpperLeftCorner
Vertex Entry Direction		Counterclockwise
Coordinate System		World
Daylighting Reference Point Coordinate System		
Rectangular Surface Coordinate System		

Figure 3.6 Zone Inputs (top) and Global Inputs (bottom)

### 3.9 Material, Construction and Surface Detailing Inputs

The material inputs of the building envelope (wall, ceiling, floor, roof, ceiling, door and window) and the construction layer are described in this section. In addition, the PCM material input and the surface details are also explained.

#### 3.9.1 Material Inputs

The material property used in the building envelope except the windows are mentioned in this class list. The required inputs are surface roughness, thickness ( $m$ ), conductivity ( $W/m-K$ ), density ( $kg/m^3$ ), specific heat ( $J/kg-K$ ), thermal absorptance, solar absorptance and visible absorptance. Most of the material values are taken from *ASHRAE Handbook- Fundamentals* and from the

datasets available in EnergyPlus. The PCM inputs are also provide here. Fig 3.7 shows the building material inputs.

Field	Units	Obj1	Obj2	Obj3	Obj4	Obj5	Obj6	Obj7	Obj8	Obj9	Obj10	Obj11	Obj12	Obj13	Obj14
Name		Composite 2x4 Wood Stud R13 #2	Composite 2x6 Wood Stud R19 #2	Concrete	Door	1/2" OSB Roof Sheathing	Roofing Felt	Fiberglass Desert Tan Shingles	T111 Siding Door	Gypsum Board	Ceiling Siding	Floor	BioPCM FLOOR	BioPCM CEILING	BioPCM WALL
Roughness		Smooth	Smooth	MediumRough	MediumRough	Smooth	Smooth	Smooth	Smooth	Smooth	Smooth	Smooth	Smooth	Smooth	Smooth
Thickness	m	0.083	0.133	0.1016	0.033	0.0127	0.0127	0.0127	0.0127	0.0127	0.0127	0.0508	0.010186	0.010186	0.0020182
Conductivity	W/m-K	0.0445	0.047	2.15	0.1	0.15	1.2	0.15	0.1	0.16	0.1	0.1	0.2	0.2	0.2
Density	kg/m3	119.63	93.84	2400	500	600	2250	600	500	640	500	500	860	860	860
Specific Heat	J/kg-K	1049	1006	900	1880	1000	1260	1000	1880	1150	1880	1880	1620	1620	1620
Thermal Absorptance		0.9	0.9	0.9	0.9	0.9	0.9	0.9	0.9	0.9	0.9	0.9	0.9	0.9	0.9
Solar Absorptance		0.7	0.7	0.7	0.78	0.7	0.7	0.7	0.78	0.75	0.78	0.7	0.7	0.7	0.7
Visible Absorptance		0.7	0.7	0.7	0.78	0.7	0.7	0.7	0.78	0.75	0.78	0.7	0.7	0.7	0.7

Figure 3.7 Building Material Inputs

The window material chosen was clear 6mm glass available in the EnergyPlus dataset. The inputs of the window are shown in Fig 3.8.

Field	Units	Obj1
Name		CLEAR 6MM
Optical Data Type		SpectralAverag
Window Glass Spectral Data Set Name		
Thickness	m	0.006
Solar Transmittance at Normal Incidence		0.775
Front Side Solar Reflectance at Normal Incidence		0.071
Back Side Solar Reflectance at Normal Incidence		0.071
Visible Transmittance at Normal Incidence		0.881
Front Side Visible Reflectance at Normal Incidence		0.08
Back Side Visible Reflectance at Normal Incidence		0.08
Infrared Transmittance at Normal Incidence		0
Front Side Infrared Hemispherical Emissivity		0.84
Back Side Infrared Hemispherical Emissivity		0.84
Conductivity	W/m-K	0.9
Dirt Correction Factor for Solar and Visible Transmittance		
Solar Diffusing		

Figure 3.8 Window Inputs

The user has to supply the enthalpy data for the phase change material in addition to the thickness, thermal conductivity, density and specific heat capacity. This is supplied in tabular form as in Table 3.4

Table 3.4 Enthalpy-Temperature Input

Temp (°C)	Enthalpy (J/kg)	Temp (°C)	Enthalpy (J/kg)
0	14.10	29	80168.01
5	7034.67	30	208169.50
10	14364.05	31	246573.79
15	22079.84	33	250241.32
20	30267.74	35	253659.41
25	39919.57	40	262147.38
27	46366.20	45	270457.58
28	53607.46	50	278158.96

### 3.9.2 Construction Inputs

The construction class list describes the various layers in the building envelope starting from the outermost layer to the innermost layer. The Fig 3.8 is for the PCM shed. For the non PCM shed, the PCM layers are removed.

Field	Units	Obj1	Obj2	Obj3	Obj4	Obj5	Obj6	Obj7
Name		Floor - Attic	Door	Roof	Window	Ceiling	Floor	Wall
Outside Layer		Gypsum Board	Door	Fiberglass Desert Tan Shingles	CLEAR 6MM	Ceiling Siding	Concrete	T111 Siding Door
Layer 2		BioPCM CEILING		Roofing felt		Composite 2x6 Wood Stud R19 #2	Floor	Composite 2x4 Wood Stud R13 #2
Layer 3		Composite 2x6 Wood Stud R19 #2		1/2" OSB Roof Sheathing		BioPCM CEILING	BioPCM FLOOR	BioPCM WALL
Layer 4		Ceiling Siding				Gypsum Board	Floor	Gypsum Board
Layer 5								
Layer 6								
Layer 7								
Layer 8								
Layer 9								
Layer 10								

Figure 3.9 Construction Input

### 3.9.3 Surface Detailing

The surface detailing class list pictured in Fig 3.10 describes each surface of the construction. It defines the dimension of the surface with respect to origin, zone to which it belongs, construction layer, type of surface, outside boundary condition, view factors to ground and exposure to ambient conditions. It has to be noted that the floor has been set to ground to facilitate ground heat transfer.

Field	Units	Obj1	Obj2	Obj3	Obj4	Obj5	Obj6	Obj7	Obj8	Obj9	Obj10	Obj11	Obj12
Name		Attic - Roof	Attic - Floor	Wall - West	Wall - North	Wall - South	Wall - East	Living Ceiling	Floor	Attic - North	Attic - South	Attic - East	Attic - West
Surface Type		Roof	Floor	Wall	Wall	Wall	Wall	Ceiling	Floor	Wall	Wall	Roof	Roof
Construction Name		Roof	Ceiling	Wall	Wall	Wall	Wall	Ceiling	Floor	Wall	Wall	Roof	Roof
Zone Name		Attic	Attic	Living Zone	Living Zone	Living Zone	Living Zone	Living Zone	Living Zone	Attic	Attic	Attic	Attic
Outside Boundary Condition		Outdoors	Surface	Outdoors	Outdoors	Outdoors	Outdoors	Surface	Ground	Outdoors	Outdoors	Outdoors	Outdoors
Outside Boundary Condition Object			Living Ceiling					Attic - Floor					
Sun Exposure		SunExposed	NoSun	SunExposed	SunExposed	SunExposed	SunExposed	NoSun	NoSun	SunExposed	SunExposed	SunExposed	SunExposed
Wind Exposure		WindExposed	NoWind	WindExposed	WindExposed	WindExposed	WindExposed	NoWind	NoWind	WindExposed	WindExposed	WindExposed	WindExposed
View Factor to Ground		autocalculate	autocalculate	autocalculate	autocalculate	autocalculate	autocalculate	autocalculate	autocalculate	autocalculate	autocalculate	autocalculate	autocalculate
Number of Vertices		3								3			
Vertex 1 X-coordinate	m	1.825	0	0	3.657	0	3.657	0	0	1.825	1.825	1.825	1.825
Vertex 1 Y-coordinate	m	0	0	4.876	4.876	0	0	4.876	0	4.876	0	0	4.876
Vertex 1 Z-coordinate	m	3.2894	2.436	2.436	2.436	2.436	2.436	2.436	0	3.2894	3.2894	3.2894	3.2894
Vertex 2 X-coordinate	m	1.825	0	0	3.657	0	3.657	0	0	3.657	0	3.657	0
Vertex 2 Y-coordinate	m	2.436	4.876	4.876	4.876	0	0	0	4.876	4.876	0	0	4.876
Vertex 2 Z-coordinate	m	3.2894	2.436	0	0	0	0	2.436	0	2.436	2.436	2.436	2.436
Vertex 3 X-coordinate	m	1.825	3.657	0	0	3.657	3.657	3.657	3.657	0	3.657	3.657	0
Vertex 3 Y-coordinate	m	4.876	4.876	0	4.876	0	4.876	0	4.876	4.876	0	4.876	0
Vertex 3 Z-coordinate	m	3.2894	2.436	0	0	0	2.436	0	2.436	2.436	2.436	2.436	2.436
Vertex 4 X-coordinate	m		3.657	0	0	3.657	3.657	3.657	3.657			1.825	1.825
Vertex 4 Y-coordinate	m	0	0	4.876	0	4.876	4.876	0				4.876	0
Vertex 4 Z-coordinate	m		2.436	2.436	2.436	2.436	2.436	0				3.2894	3.2894
Vertex 5 X-coordinate	m												
Vertex 5 Y-coordinate	m												

Figure 3.10 Building Surface Detailed

Field	Units	Obj1	Obj2
Name		Door	Windows - East
Surface Type		Door	Window
Construction Name		Door	Window
Building Surface Name		Wall - East	Wall - East
Outside Boundary Condition Object			
View Factor to Ground		autocalculate	autocalculate
Shading Control Name			
Frame and Divider Name			
Multiplier		1	1
Number of Vertices		4	4
Vertex 1 X-coordinate	m	3.657	3.657
Vertex 1 Y-coordinate	m	1.6764	2.7432
Vertex 1 Z-coordinate	m	2.1336	2.1336
Vertex 2 X-coordinate	m	3.657	3.657
Vertex 2 Y-coordinate	m	1.6764	2.7432
Vertex 2 Z-coordinate	m	0.1524	1.646
Vertex 3 X-coordinate	m	3.657	3.657
Vertex 3 Y-coordinate	m	2.4384	3.5052
Vertex 3 Z-coordinate	m	0.1524	1.646
Vertex 4 X-coordinate	m	3.657	3.657
Vertex 4 Y-coordinate	m	2.4384	3.5052
Vertex 4 Z-coordinate	m	2.1336	2.1336

3.11 Fenestration Surface Detailed

The fenestration surface detailing shown in Fig 3.11 is similar to the previous class list. The only additional input is to mention the surface on which it is located.



### 3.10 HVAC Inputs

The HVAC system used in the experiment was a window mounted heat pump manufactured by AMAMA. Packaged terminal heat pump module was used in EnergyPlus simulation. This module requires input for the following five elements:

1. Outdoor air mixer
2. DX Cooling coil element
3. DX Heating coil element
4. Fan (draw through fan)
5. Supplemental heater

The following Fig 3.12 depicts the heat pump configuration

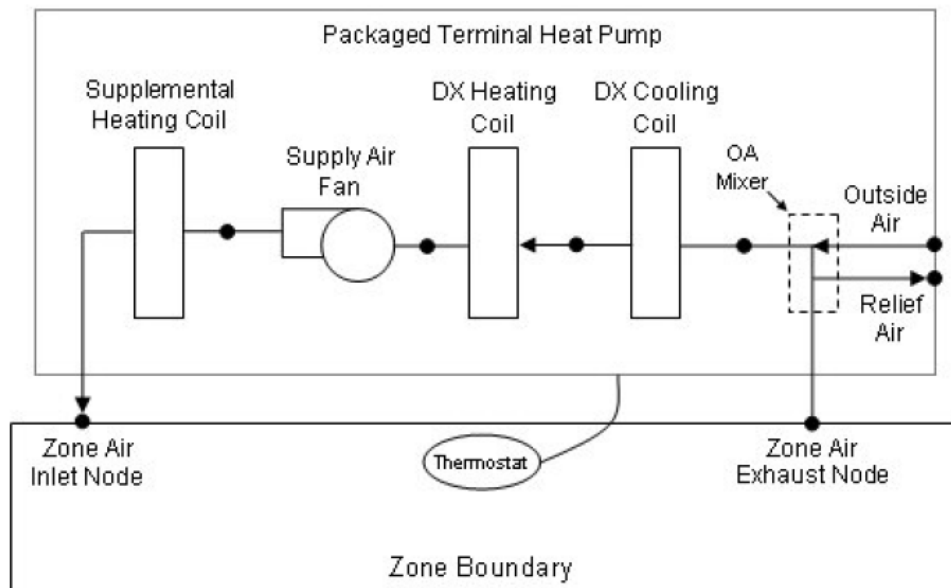


Figure 3.12 Schematic of Packaged Terminal Heat Pump

(Source: EnergyPlus documentation)

### 3.10.1 Outdoor Air Mixer

The outdoor air mixer is a passive component. It has two inlets: system return air and outdoor air. The two outlet air streams are: system relief air and the mixed air. The heat pump used in the experimental setup does not have an outdoor air mixer. The outdoor air enters the zone through infiltration. Hence dummy node names are assigned for the simulation and the outdoor air flow rate during heating, cooling and no heating/cooling has been set to 0 m<sup>3</sup>/s. The Fig 3.13 below shows outdoor air mixer class list.

Field	Units	Obj1
Name		Outdoor Air Mixer
Mixed Air Node Name		Outdoor Air Mixer Node
Outdoor Air Stream Node Name		Outdoor Air Inlet Node
Relief Air Stream Node Name		Relief Air Outlet Node
Return Air Stream Node Name		PTHP Inlet Node

Figure 3.13: Outdoor Air Mixer Class List in EnergyPlus

### 3.10.2 DX Cooling Coil

The two types of DX cooling coil available in EnergyPlus are single speed and two speeds. The packaged terminal heat pump in our case uses single speed DX cooling coil. The inputs of the cooling coil are: availability schedule, air inlet node name, air outlet node name, performance curve details, rated total cooling capacity, rated sensible heat ratio, rated COP, and rated air flow rate. The last 4 inputs determine the coil performance at the rating point

The model used performance information at rated conditions along with curve fits for variation in total capacity, energy input ratio and part-load fraction to

determine performance at part-load conditions. Since the heat pump used in the experimental setup is a smaller capacity model, it runs either at full-load or no-load conditions. The cooling performance curves are explained in detail in later section. The cooling coil inputs in EnergyPlus illustrated in Fig 3.14

Field	Units	Obj1
Name		Heat Pump Cooling Coil
Availability Schedule Name		CoolingCoilAvailSch ed
Rated Total Cooling Capacity	W	2726
Rated Sensible Heat Ratio		0.75
Rated COP		2.93
Rated Air Flow Rate	m3/s	0.15
Rated Evaporator Fan Power Per Volume Flow Rate	W/(m3/s)	0
Air Inlet Node Name		Outdoor Air Mixer Node
Air Outlet Node Name		Heating Coil Inlet Node
Total Cooling Capacity Function of Temperature Curve Name		HPACCoolCapFT
Total Cooling Capacity Function of Flow Fraction Curve Name		HPACCoolCapFFF
Energy Input Ratio Function of Temperature Curve Name		HPACEIRFT
Energy Input Ratio Function of Flow Fraction Curve Name		HPACEIRFFF
Part Load Fraction Correlation Curve Name		HPACPLFFPLR

Figure 3.14 DX Cooling Coil Inputs 1

### 3.10.3 DX Heating Coil

Similarly to the cooling coil, the DX heating coil has two variations: single speed and two speeds. The AMANA heat pump uses a single speed DX heating coil. The inputs required are: availability schedule, air inlet node name, air outlet node name, rated total heating capacity, rated COP and the rated air volume flow rate. The last 3 inputs determine the coil performance at the rating condition.

The single speed heating DX coil model uses performance information at rated conditions along with curve fits for variations in total capacity, energy input ratio and part load fraction to determine performance at part-load conditions.

Since the heat pump used in our setup is a smaller capacity model, it runs either at full-load or no-load conditions. The heating performance curves are explained in detail in later section. The heating coil inputs in EnergyPlus are illustrated in Fig 3.15.

Field	Units	Obj1
Name		Heat Pump Heating Coil
Availability Schedule Name		HeatingCoilAvailSchedule
Rated Total Heating Capacity	W	2462
Rated COP		2.8
Rated Air Flow Rate	m3/s	0.14
Air Inlet Node Name		Heating Coil Inlet Node
Air Outlet Node Name		Heating Coil Outlet Node
Total Heating Capacity Function of Temperature Curve Name		HPACHeatCapFT
Total Heating Capacity Function of Flow Fraction Curve Name		HPACHeatCapFFF
Energy Input Ratio Function of Temperature Curve Name		HPACHeatEIRFT
Energy Input Ratio Function of Flow Fraction Curve Name		HPACHeatEIRFFF
Part Load Fraction Correlation Curve Name		HPACCOOLPLFFPLR

Figure 3.15 DX Heating Coil Inputs

#### 3.10.4 Fan

The heat pump uses a constant volume fan that cycles on and off along with the compressor operation. The Fig 3.16 shows the required inputs and the corresponding values. The motor in airstream fraction defines the fraction of motor heat added to the air stream. It varies from 0 to 1. Since the fan used in this heat pump is located outside the air stream, zero is taken as the input.

Field	Units	Obj1
Name		Heat Pump Fan
Availability Schedule Name		FanAndCoilAvailSchedule
Fan Efficiency		0.6
Pressure Rise	Pa	75
Maximum Flow Rate	m3/s	0.15
Motor Efficiency		0.9
Motor In Airstream Fraction		0
Air Inlet Node Name		Heating Coil Outlet Node
Air Outlet Node Name		Fan Outlet
Fan Power Ratio Function of Speed Ratio Curve Name		
Fan Efficiency Ratio Function of Speed Ratio Curve Name		
End-Use Subcategory		

Figure 3.16 Fan Inputs

### 3.10.5 Supplemental Heater

Supplemental heater is used in addition to the reversed cycle heat pump. It operates when the capacity of the heating coil is insufficient to meet the heating loads. The required inputs are: availability schedule, efficiency, nominal capacity, air inlet node name and air outlet node name. Fig 3.17 depict the electric heater inputs.

Field	Units	Obj1
Name		Heat Pump Supp Heating
Availability Schedule Name		HeatingCoilAvailSchedule
Efficiency		0.8
Nominal Capacity	W	3136
Air Inlet Node Name		Fan Outlet
Air Outlet Node Name		PTHP Exhaust Node
Temperature Setpoint Node Name		

Figure 3.17 Electric Heater Inputs

### 3.10.6 Infiltration, Ventilation and Thermostat Inputs

Infiltration is the uncontrolled flow of air from outside environment to the zone through cracks and openings in the building's envelope. The infiltration used in the EnergyPlus simulation is based on Effective Leakage Area Model. This model is appropriate for smaller residential-type buildings and for single-zone buildings without mechanical ventilation. The equation used to calculate infiltration using effective leakage area model is:

$$Infiltration = \frac{A_L}{1000} \sqrt{C_s \Delta T + C_w (WindSpeed)^2} \quad (3.8)$$

where,

$A_L$  - Effective leakage area,  $cm^2$

$\Delta T$  - Average difference between zone air temperature and the outdoor air temperature

$C_s$  - Stack coefficient,  $(L/s)^2/(cm^4.K)$

- 0.000145  $(L/s)^2/(cm^4.K)$  for one story house

$C_w$  - Wind coefficient,  $(L/s)^2/[cm^4.(m/s)^2]$

- 0.000319  $(L/s)^2/[cm^4.(m/s)^2]$  for one story house with no obstructions or local shielding

The effective leakage area is calculated as shown in Table 3.4. The leakage area per area or perimeter values is taken from *ASHRAE Handbook - Fundamentals*.

The attic ventilation is provided by two rectangular louvered vents installed in each shed. An air flow rate of 0.01  $m^3/s$  was assumed and other inputs was taken as default values.

The thermostat input used in EnergyPlus was dual set point thermostat as it can provided heating or cooling at any time during the day depending on the requirements.

Table 3.5 Zone Infiltration Calculation

Component	Perimeter (m) or Area (m <sup>2</sup> )	Leakage Area Per Area (cm <sup>2</sup> /m <sup>2</sup> ) OR Perimeter (cm <sup>2</sup> /m)	Leakage Area (cm <sup>2</sup> )
Walls at sill (sill uncaulked)	17 m	4 cm <sup>2</sup> /m	68
Walls at roof (not taped or plastered, no vapor barrier)	17 m	1.5 cm <sup>2</sup> /m	25.5
Windows (Single-hung, not weather-stripped)	0.371 m <sup>2</sup>	2.2 cm <sup>2</sup> /m <sup>2</sup>	0.816
Window frames (no caulking)	0.371 m <sup>2</sup>	1.7 cm <sup>2</sup> /m <sup>2</sup>	0.6307
Door (Single door)	1.5 m <sup>2</sup>	7.86 cm <sup>2</sup> /m <sup>2</sup>	11.79
Door frame (no caulking)	1.5 m <sup>2</sup>	1.66 cm <sup>2</sup> /m <sup>2</sup>	2.5
Effective leakage area			109.23

### 3.11 Performance Curves (Source: EnergyPlus Documentation)

#### 3.11.1 Cooling Coil

The performance curve details of the cooling coil are described below. All these curves are normalized to have a value of 1.

- Total Cooling Capacity Function of Temperature Curve

It is a biquadratic performance curve that models the variation of the total cooling capacity as a function of the wet-bulb temperature and the dry-bulb temperature. The total cooling capacity at particular operating point is obtained by multiplying the output of this curve with the rated total cooling capacity.

- Total Cooling Capacity Function of Flow Fraction Curve

This performance curve is quadratic or cubic in nature. It parameterizes the variation of total cooling capacity as a function of the ratio of actual air flow rate across the cooling coil to the rated air flow rate (at full load conditions). The total cooling capacity at specific operating conditions is a product of the curve's output, rated total cooling capacity and total cooling capacity modifier curve.

- Energy Input Ratio Function of Temperature Curve

This is a biquadratic performance curve that represents the energy input ratio (EIR) as a function of the wet-bulb and the dry-bulb temperature. The EIR at specific operating conditions is obtained by multiplying the output of the curve with the rated EIR (inverse of rated COP).



- Energy Input Ratio Function of Flow Fraction Curve

This is a quadratic or cubic curve that characterizes energy input ratio (EIR) as dependent on the ratio of actual air flow rate across the cooling coil to the rated air flow rate (at full load conditions). The EIR is the inverse of the COP. The output of this curve is multiplied by the rated EIR and the EIR modifier curve (function of temperature) to give the EIR at the specific conditions.

- Part Load Fraction Correlation Curve

This curve which is in form of quadratic or cubic equation models the electrical power input variation to the DX unit as a function of the part load ratio (PLR). The effective EIR at a particular simulation timestep is obtained by dividing the product of the rated EIR and EIR modifier curves by the output of the curve. The part load fraction (PLF) signifies losses in efficiency due to cyclic compressor operation.

### 3.11.2 Heating Coil

The performance curves of the heating coil are described below. All these curves are normalized to have a value of 1.

- Total Heating Capacity Function of Temperature Curve

This bi-quadratic, quadratic or cubic performance curve models the total heating capacity as a function of the both the indoor and outdoor air dry-bulb temperature or just the outdoor air dry-bulb temperature. The product of the curve's output and rated total heating capacity gives the total heating capacity at specific operating conditions

- **Total Heating Capacity Function of Flow Fraction Curve**

This curve is in form of a quadratic or cubic equation. It characterizes the total heating capacity which depends on the ratio of actual air flow rate across the heating coil to the rated air flow rate (i.e., at full load conditions). The total heating capacity at particular operating conditions is obtained as product of the curve's output, rated total heating capacity and the total heating capacity modifier curve (function of temperature).
- **Energy Input Ratio Function of Temperature Curve**

This curve illustrates energy input ratio (EIR) as a dependent variable of either the indoor and outdoor air dry-bulb temperature or just the outdoor air dry-bulb temperature. The result of this curve is multiplied by the rated EIR (inverse of rated COP) to give the EIR at specific temperature operating conditions. This performance curve can be of bi-quadratic, quadratic or cubic form.
- **Energy Input Ratio Function of Flow Fraction Curve**

This performance curve (quadratic or cubic) parameterizes the variation of the energy input ratio (EIR) as a function of the ratio of actual air flow rate across the heating coil to the rated air flow rate. The output of this curve is multiplied by the rated EIR and the EIR modifier curve (function of temperature) to give the EIR at the specific operating conditions.
- **Part Load Fraction Correlation Curve**

This curve which is in form of quadratic or cubic equation models the electrical power input variation to the DX unit as a function of the part load ratio (PLR). The effective EIR at a particular simulation timestep is

obtained by dividing the product of the rated EIR and EIR modifier curves is by the output of the curve. The part load fraction (PLF) represents efficiency losses due to compressor cycling.

### 3.12 Simulation Work Carried Out

In EnergyPlus the following simulation work was carried out.

- a. Simulation of PCM and Non PCM shed with inputs like material, construction, HVAC system, location, weather file closely matching with the experimental setup. The aim is to observe the trend of energy savings and peak load time shift.

- b. Parametric studies:

Other studies were carried out to maximize the building performance using PCM for Phoenix location.

- Variation of thermal conductivity of the PCM
- Variation of the PCM temperature range.
- Variation of location of the PCM layer
- Variation of the R-value of the insulation of the wall
- Variation of the PCM temperature range only in the west and south wall.

## Chapter 4

### RESULTS AND DISCUSSION

#### 4.1 Overview

This chapter discusses the results obtained in the experimental setup and simulation using EnergyPlus. It also analysis the various parametric studies carried out to maximize building performance using PCM.

#### 4.2 Thermal Resistance of the Wall with PCM and without PCM

To confirm that the addition of PCM does not cause significant increase in thermal resistance, a simple computation is done to calculate the effective thermal resistance of wall with PCM and the wall without PCM. The thermophysical properties of the materials are obtained from *ASHRAE handbook - Fundamentals*.

##### 4. 1 Thermal Resistance of the Wall Without PCM

R VALUE CALCULATION OF THE WALL WITHOUT PCM							
ELEMENTS	Heat Tranfer Co-eff	Thermal Conductivity	Thickness (L)	Area (A)	R value	R Formula	R
	W/(m2.K)	W/(m*K)	m	m2	K.m2/W	K/W	K/W
Outside Environment	28.39	-	-	0.1394	-	$1/(h_o * A)$	0.253
T111 Siding	-	0.1	0.0127	0.1394	-	L/KA	0.911
Wood Stud	-	0.125	0.102	0.0155	-	$1/(((2 * K * A) / L) + (A / R_{ins}))$	11.717
Insulation	-			0.1084	2.289		
Gypsum Board	-	0.16	0.0127	0.1394	-	L/KA	0.569
Inside Environment	8.289			0.1394	-	$1/(h_i * A)$	0.865
						Rtotal	14.315

The formula used to compute the wall's resistance without PCM is

$$R_{PCM} = R_{CONV1} + R_{T111} + \frac{1}{\frac{1}{R_{WOOD1}} + \frac{1}{R_{INS}} + \frac{1}{R_{WOOD2}}} + R_{GYPSUM} + R_{CONV2} \quad (4.1)$$

Similarly, for the shed with PCM, the resistance formula is

$$R_{NONPCM} = R_{CONV1} + R_{T111} + \frac{1}{\frac{1}{R_{WOOD1}} + \frac{1}{R_{INS}} + \frac{1}{R_{PCM}} + \frac{1}{R_{WOOD2}}} + R_{GYPSUM} + R_{CONV2} \quad (4.2)$$

#### 4. 2 Thermal Resistance of the Wall With PCM

R VALUE CALCULATION OF THE WALL WITH PCM							
ELEMENTS	Heat Transfer Co-eff	Thermal Conductivity	Thickness (L)	Area (A)	R value	R Formula	R
	W/(m2.K)	W/(m*K)	m	m2	K.m2/W	K/W	K/W
Outside Environment	28.39	-	-	0.1394	-	1/(ho*A)	0.253
T111 Siding	-	0.1	0.0127	0.1394	-	L/KA	0.911
Wood Stud	-	0.125	0.102	0.0155	-	1/(((2*K*A)/L)+(1/((L/K*A)+(Rins/A))))	11.745
Insulation	-			0.1084	2.289		
BioPCM Mat		0.2	0.002	0.1084	-		
Gypsum Board	-	0.16	0.0127	0.1394	-	L/KA	0.569
Inside Environment	8.289			0.1394	-	1/(hi*A)	0.865
Rtotal							14.344

The thermal resistances of the shed with PCM and without PCM are 14.344 K/W and 14.315 K/W respectively considering same cross-sectional area for both cases and neglecting the plastic encapsulation of the BioPCM for the PCM shed. The increase in the thermal resistance with PCM is just 0.2 % and hence the energy savings and peak load time shift can be attributed solely to the

heating storing and releasing property of the PCM. The thermal resistance for the shed with PCM was calculated assuming a continuous of PCM without any air gap and neglecting the resistance of the plastic encapsulation.

In the EnergyPlus simulation, the inside surface convection algorithm used was ASHRAE –detailed (i.e. variable natural convection based on temperature difference). The minimum and maximum inside heat transfer coefficient,  $H_i$  used was 0.1 and 2.36 W/m<sup>2</sup>-K. Hence the resistance ( $1/H_i$ ) varies from 10 to 0.423 m<sup>2</sup>-K/W. On the other hand, the wall BioPCM (thickness = 0.002 m, thermal conductivity = 0.2 W/m-k) had a thermal resistance of 0.1 m<sup>2</sup>-K/W. Hence the magnitude of the convective resistance varies 4 to 100 times that of the BioPCM resistance. In actual case, the BioPCM would have slightly higher thermal resistance because the air gap acts as a better insulator.

#### 4.3 Experimental Results

The actual data collected at the experimental site were analyzed and energy savings, time shift in occurrence of peak load, cost savings and reduction in energy demand during on-peak hours are discussed.

The following are the technical difficulties faced during the experiment.

- The door of the shed had blown open and was replaced in January 2008.
- 50% of the wall PCM was replaced with identical density on June 21<sup>st</sup> 2008 due to film issues.
- Two attic vents were installed in each shed on June 21<sup>st</sup> 2008
- Programmable thermostats were installed on May 30<sup>th</sup> 2008.

- The experimental data was initially recorded for 10 min for the months (January, February, March and December) and 1 min for the remaining months.
- The actual data was available only for 291 days out of 366.

#### 4.3.1 Energy Consumption and Peak Load Shift

Table 4.3 summarizes the peak load shift and the monthly energy usage calculated for all the months from the experimental data. The peak load was calculated by taking the 15 min average of the time derivative of the energy usage, kWh for the given month.

4. 3 Energy Usage and Peak Load Shift

Month	Valid Data Days	Time Interval Between Recorded Data (min)	Peak Load Shift		Monthly kWh Energy Usage		
			Yes/No	Time Shift (min)	Without PCM (kWh)	With PCM (kWh)	Savings (%)
Jan	24	10	No	-	157.193	111.897	28.82
Feb	28	10	No	-	113.551	91.364	19.54
Mar	30	10	No	-	92.421	83.919	9.2
Apr	24	1	No	-	95.727	81.526	14.83
May	15	1	No	-	126.217	108.618	13.94
Jun	25	1	Yes	60	273.204	240.165	12.09
Jul	22	1	Yes	-	318.775	268.152	15.88
Aug	27	1	Yes	-	292.695	234.417	19.91
Sept	26	1	Yes	3	188.927	140.031	25.88
Oct	30	1	No	2	94.104	71.272	24.26
Nov	22	1	No	-	60.209	42.595	29.25
Dec	18	10	No	-	152.988	116.219	24.03

For example, consider the month of June which has experimental data for 25 days with data being collected every minute for both the sheds. First, the energy usage, kWh is normalized for the first data available day. That is, the difference between the second kWh reading and first kWh reading, third kWh

reading and first kWh reading, fourth kWh reading and first kWh reading and so on are calculated. Secondly, the energy usage values are normalized for all the data available days. We have time on first column, normalized energy usage of first day in second column, normalized energy usage for second day in third column and so on. Then we sum the energy usage for a given minute, which is adding all the values horizontally and storing the value in the last column. Then we divide the summed value by the number of data available days. To find power for the first minute, we subtract the second kWh reading from the first kWh reading and multiply by 60 to convert kWh to kW. Similarly, it is done for the remaining minutes in a day. Finally, it is also done for the other shed. We obtained several fluctuations for 1 min duration as seen in Fig 4.1.

Figures 4.1 – 4.4 present the 1 min and 15 min average peak loads for the summer months in 2008, for both the North (with BioPCM) and South (no BioPCM) sheds.

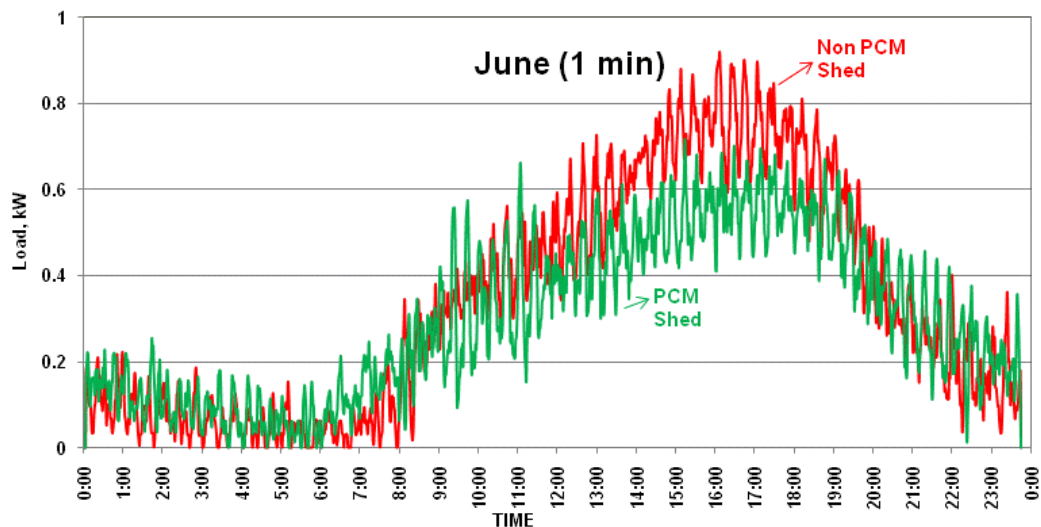


Figure 4.1 Experimental Peak Curve for June (1 min)



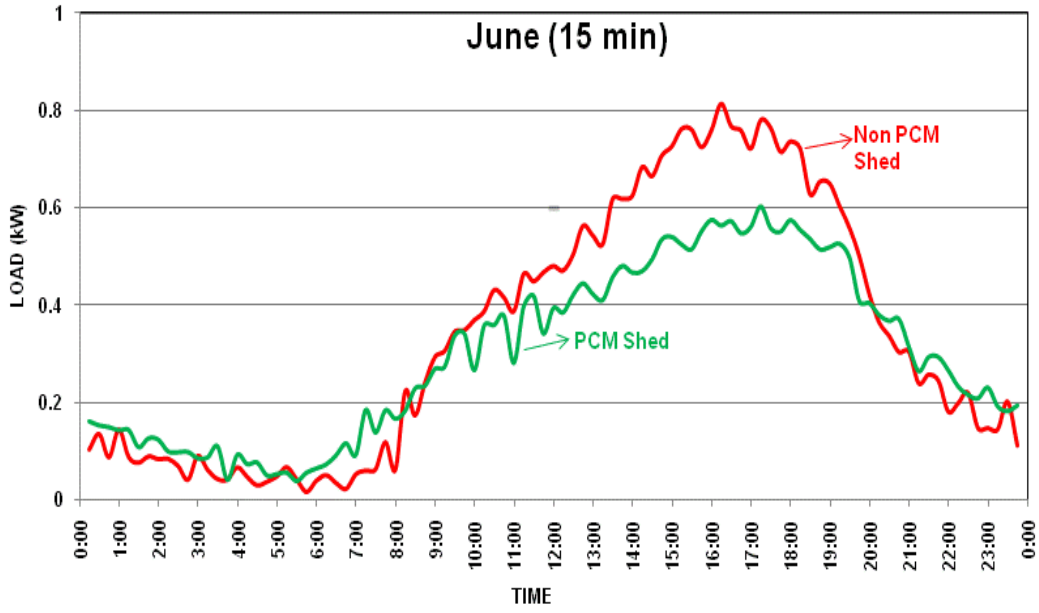


Figure 4.2 Experimental Peak Curve for June (15 min)

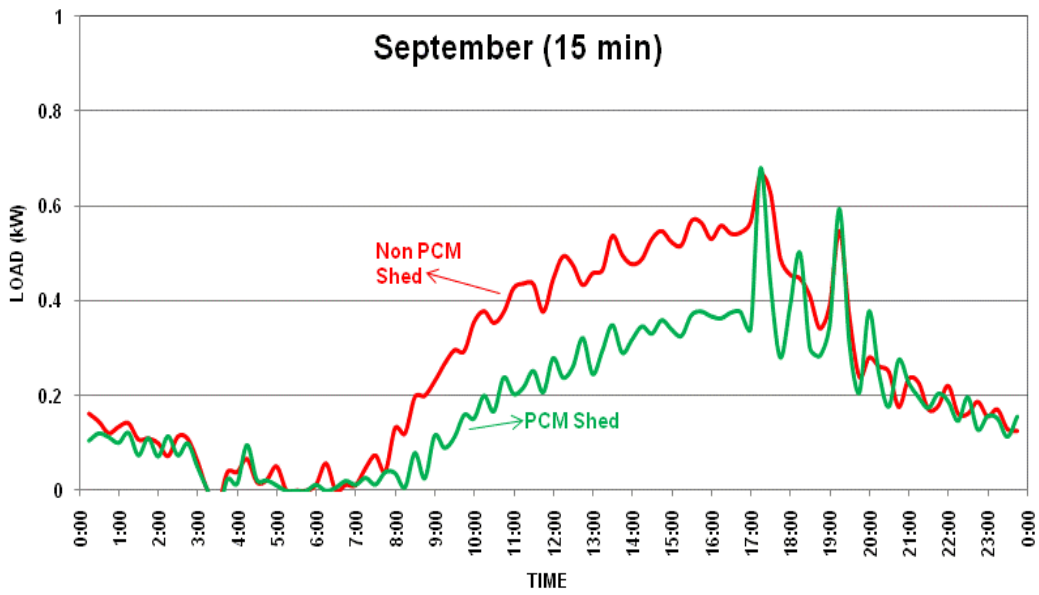


Figure 4.3 Experimental Peak Curve for September (15 min)

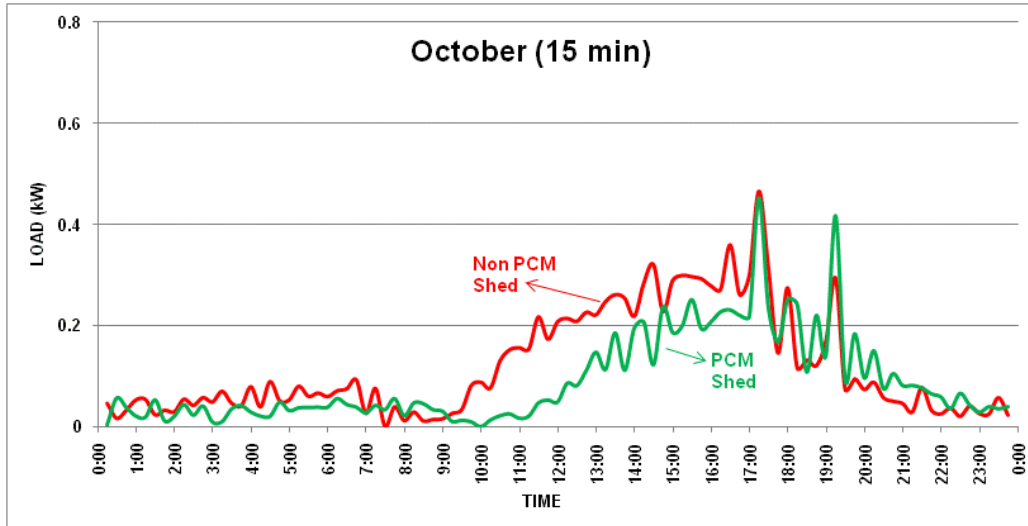


Figure 4.4 Experimental Peak Curve for October (15 min)

The red and green curve indicates the shed without PCM and with PCM respectively. The peak shift is observed to take place between 4:00 PM to 5:15 PM, the time of intense insolation and high ambient temperature in Tempe, Arizona. The time duration between the peak load of two sheds shows the shift time. The time shift in peak power consumption was seen only for few of the summer months (June, September and October). The maximum time shift occurred in June (60 min), and the minimum for the summer occurred in October (2 min). The possible reasons for no peak-load time shift during the other months of the year might be due to very shorter time frame involving phase change transition of the PCM.

The energy savings were highest for the month of November with nearly 30% while March recorded the least value of about 9%. Referring to the NREL [13] weather data for Phoenix, it was observed that some winter months (Jan, Feb, and Dec) had no days and other months (Mar & Nov) had few days with

ambient temperature above the melting point of the PCM. So it can be concluded that the solar radiation would have been the prime factor to cause considerable phase change during winter.

The energy savings during winter months can be attributed due to partial melting (solid and liquid phase) of the PCM in shorter duration (noon till evening) by moderate ambient temperature or by mild solar radiation or both. The solid-liquid transition phase change have the highest heat capacity and would have aided in storing thermal energy thereby preventing passage of heat to the interior. The solidification of the PCM takes places later in the evening by discharging heat to the interior of the shed. This additional heat liberated by the PCM helps in heating the shed, thus reducing work load on the heat pump unit.

From the experimental data in Fig 4.2 to 4.4, it can be observed that little fluctuations occurred during the early mornings and late nights indicating the additional work done by the HVAC unit to keep the shed at the desired comfort temperature. This is due to the discharge process of the BioPCM during which heat is released both inside and outside the shed. The additional heat released by the PCM has to be removed by the heat pump thereby consuming more power which causes oscillations in the curve. This increased air conditioning load during the night time can possibly be reduced by removing heat from the BioPCM by flowing tap water through copper tubes in contact with the BioPCM, as suggested by Pasupathy et al. [5] The percentage reduction in peak load due to PCM are also calculated in Table 4.4. The maximum reduction is close to 27% (July) and least value is about 7% (October).

#### 4.4 Percentage Reduction in Peak Load

Month	Shed	Time (hh:mm)	Load (kW)	Reduction in Peak Load (%)	Time Shift (min)
June	Non PCM	16:00	0.812	25.67	60
	PCM	17:00	0.604		
July	Non PCM	17:00	0.874	26.93	NA
	PCM	16:15	0.638		
August	Non PCM	17:00	0.850	16.48	NA
	PCM	17:00	0.710		
September	Non PCM	17:03	0.907	NA	3
	PCM	17:06	0.921		
October	Non PCM	17:04	0.826	7.02	2
	PCM	17:06	0.768		

#### 4.3.2 Cost Savings and Reduction in Energy Demand (On-Peak Hours)

To accurately calculate cost savings, billing cycles adopted in Arizona were used. Different billing cycles (Tables 4.5 and 4.6) are used for on-peak hours (9:00 AM to 9:00 PM) and off-peak hours (9:00 PM to 9:00 AM). The billing cycle is varied also for different classes of residential and business establishments and also for summer and winter seasons. It can be noted that the summer and on-peak hours are priced slightly higher than their counterparts as expected due to higher demand during those time of the year.

Table 4.5 Residential Billing Cycle

Billing Cycles	Residential Rates	
	On-Peak Hours	Off-Peak Hours
	(9:00 AM to 9:00 PM)	(9:00 PM to 9:00 AM)
Summer (May to Oct)	\$0.1581 per kWh	\$0.0511 per kWh
Winter (Nov to Apr)	\$0.12845 per kWh	\$0.04925 per kWh

Table 4.6 Business Billing Cycle

Billing Cycles	Business Rates	
	On-Peak Hours	Off-Peak Hours
	(9:00 am to 9:00 pm)	(9:00 pm to 9:00 am)
Summer (May to Oct)	\$0.14329 per kWh	\$0.10607 per kWh
Winter (Nov to Apr)	\$0.12847 per kWh	\$0.09124 per kWh

Table 4.7 presents the potential cost savings for this small shed realized by employing BioPCM. A maximum percentage cost savings of about 30% (October) was observed at the residential utility rate, and 28% (November) was observed at the business utility rate. This suggests that the currently employed BioPCM with melting point of 29 °C works most efficiently in the transition between summer and winter season during which less intense insolation and ambient temperatures were observed. March was found to have the least cost savings of around 10% for both the residential and business utility rate. The magnitude of the cost savings is more during the summer months whereas the percentage difference in cost savings is more during winter months. In summer months, the energy usage is more during on-peak hours and there is considerable reduction and energy shift to off-peak hours by use of PCM. In contrast, during winter months, the peak energy usage occurs during early morning and the excess heat liberated by PCM is helpful in reducing work load by heat pump.

Table 4.7 Cost Savings by BioPCM

Month	Residential Cost Savings	Business Cost Savings
	\$ (%)	\$ (%)
January	3.38 (31.28)	4.20 (28.13)
February	1.78 (18.44)	2.40 (18.55)
March	0.93 (9.60)	1.28 (10.47)
April	1.62 (14.13)	1.76 (14.62)
May	1.46 (12.97)	2.07 (13.78)
June	6.21 (16.98)	4.93 (13.57)
July	7.15 (19.25)	6.91 (16.85)
August	7.69 (21.63)	7.39 (19.54)
September	7.71 (29.19)	7.78 (27.99)
October	3.77 (29.38)	3.58 (28.08)
November	1.33 (26.66)	1.98 (28.23)
December	2.64 (25.13)	4.13 (24.34)

From cost point of view, adding insulation would be beneficial. As seen in table 4.8 for a small shed of 16' x 12' x 8' (L x W x H), the cost of the BioPCM material alone was \$2619 for area of 844 sq.ft. In addition to material cost, we also have shipping and labor cost for installing PCM. Moreover the PCM alone cannot substitute the insulation. That is, it is added to supplement the insulation.

4.8 Cost of BioPCM in the Shed

Elements	Area (sq.ft)	Cost/sq.ft	Cost (\$)
Wall - East	128	2.42	309.76
Wall - West	128	2.42	309.76
Wall- North	102	2.42	246.84
Wall - South	102	2.42	246.84
Floor	192	3.92	752.64
Ceiling	192	3.92	752.64
Total			2618.48

The annual cost savings for residential and business billing cycles are \$45.67 and \$48.41 respectively for this small shed. Hence the payback period calculates to about 57 and 54 years for the respective segments of the buildings. The annual energy consumption for the experimental PCM shed with R13 insulation is about 1590 kWh (Table 4.19) whereas in the EnergyPlus simulation for the non-PCM shed with R19 the consumption was 1724 kWh (Table 4.19).

The difference in the shed without installing PCM was only 134 kWh. The cost of R30 insulation varies from \$30 to \$60 for an approximate area of 50 sq.ft. Hence on cost basis, it is very much cheaper to have higher insulation like R19, R25 or R30 in the building envelope to achieve reduced energy consumption.

The use of BioPCM has shifted the energy usage in the on-peak hours to the off-peak hours, the values depending upon the seasonal months, by storing heat (charging process) during the day time and releasing them back in the night time (discharging process). This is highly crucial for business buildings as they are major consumers of energy during the on-peak hours in summer. This can also help cut down operation of power plants during peak hours of the day and reduce non-renewable fuel consumption, associated emissions and distribution losses.

The reductions in peak hour demand are calculated based on the formula

$$\text{Percentage Peak} = \frac{\text{On-Peak Energy Usage}}{\text{On-Peak Energy Usage} + \text{Off-Peak Energy Usage}} \quad (5.3)$$

Table 4.9 Reduction in Energy Demand during On-Peak Hours

MONTH	Energy Usage With BioPCM			Energy Usage Without BioPCM		
	On-Peak (kWh)	Off-Peak (kWh)	% Peak	On-Peak (kWh)	Off-Peak (kWh)	% Peak
January	25.26	67.18	27.33	40.47	86.27	31.93
February	30.55	59.62	33.88	37.36	73.39	33.73
March	39.23	50.46	43.74	42.75	57.8	42.52
April	54.73	22.93	70.47	63.37	27.85	69.47
May	40	67.92	37.06	45.2	80.38	35.99
June	170.74	65.48	72.28	213.76	53.84	79.88
July	152.37	115.91	56.8	195.28	123.12	61.33
August	148.3	86.4	63.19	194.69	93.4	67.58
September	101.63	51.37	66.42	146.06	64.7	69.3
October	52.16	16.06	76.46	75.13	18.8	79.99
November	14.05	28.38	33.11	18.35	41.2	30.81
December	18.89	95.63	16.49	26.19	124.75	17.35

The reduction in on-peak hour energy usage is noticeable during the summer season (June to October) for BioPCM sheds indicating potential energy savings. These results are quite consistent with the observed peak load time shift as seen in Table 4.3 Also a very small peak hour energy reduction is observed for December and January.



#### 4.4 Simulation Results Using Energyplus

Simulation was carried out using EnergyPlus for both the PCM and the non PCM sheds. The results are obtained for 3 minute time interval for all days in excel spread sheet. The data were processed to represent results on a monthly basis.

The challenges faced in the EnergyPlus simulation are mentioned below:

- The wall 2"x4" wood studs are placed 24" on center in the EnergyPlus simulation, whereas in the experimental setup the on center distance is 16".
- Performance curves of AMANA heat pump were not available from the manufacturer. Hence performance curves of similar heat pump were used.
- The experimental setup had discrete blocks of PCM in the envelope. The EnergyPlus used a continuous layer of PCM without any air gaps.
- The attic ventilation had an assumed value of 0.01 m<sup>3</sup>/s in the simulation
- Material properties used in the simulation has been taken from ASHRAE to closely match the experimental material properties

#### 4.4.1 Energy Consumption and Peak Load Shift

The Table 4.10 shows the energy savings and peak load time shift between PCM and non PCM sheds for both experimental setup and simulation using EnergyPlus.

Table 4.10 Energy Consumption and Peak Load Time Shift

Month	ENERGY USAGE (kWh)				ENERGY SAVINGS (%)		TIME SHIFT (min)	
	Non PCM		With PCM		Expt	Energy+	Expt	Energy+
	Expt	Energy+	Expt	Energy+				
Jan	157.19	75.25	111.9	68.92	28.82	8.41	0	0
Feb	113.55	57.67	91.36	47.28	19.54	18.01	0	0
Mar	92.42	71.07	83.92	42.68	9.2	39.95	0	0
Apr	95.73	117.96	81.53	83.85	14.83	28.92	0	3
May	126.22	171.22	108.62	134.14	13.94	21.66	0	0
Jun	273.2	333.26	240.17	278.63	12.09	16.39	60	0
Jul	318.78	346.29	268.15	293.71	15.88	15.18	15	0
Aug	292.7	314.11	234.42	264.29	19.91	15.86	45	0
Sep	188.93	250.46	140.03	204.59	25.88	18.31	30	0
Oct	94.1	135.44	71.27	101.89	24.26	24.77	0	9
Nov	60.21	55.67	42.6	35.26	29.25	36.66	0	0
Dec	152.99	70.29	116.22	62.25	24.03	11.45	0	0

The simulated energy consumption values are lower (almost half) during the winter months and are in reasonable agreement with the summer months. The EnergyPlus kWh values for the PCM shed are higher than the experimental data during the summer months due to continuous layer of PCM material used rather than discrete blocks. The absence of air gap between the PCM blocks allows more heat to pass into the shed during the summer months. In winter months, the insulation reduces the amount of heat conducting towards the outdoor environment and hence more heat from the PCM escapes through the gypsum board. This might be the reason for lower energy consumption during

the winter months. The time shift in the simulation was observed only for the months of Apr (3 min) and Oct (9 min).

The following parametric studies were carried out:

- a. Variation of thermal conductivity of the PCM
- b. Variation of the PCM temperature range.
- c. Variation of location of the PCM layer
- d. Variation of the R-value of the insulation of the wall
- e. Variation of the PCM temperature range only in the west and south wall.
- f. Variation of the PCM thickness

#### 4.4.2 Variation of Thermal Conductivity of the PCM

In EnergyPlus the thermal conductivity of the PCM was varied and simulation was carried out. The thermal conductivity values used were: 0.1, 0.2, 0.3, 0.4 and 0.5 W/m-K. The Table 4.11, 4.12 and 4.13 shows the energy usage, energy savings and time shift results. The PCM temperature range used for all the cases was from 27 to 31 °C and other parameters were kept constant.

Table 4.11 Variation of Thermal Conductivity of the PCM

Month	ENERGY USAGE (kWh)							
	Non PCM		With PCM					
	Expt	Energy+	Expt	Energy+ k=0.1	Energy+ k=0.2	Energy+ k=0.3	Energy+ k=0.4	Energy+ k=0.5
Jan	157.19	75.25	111.90	68.68	68.92	69.01	69.05	69.07
Feb	113.55	57.67	91.36	47.13	47.28	47.34	47.36	47.37
Mar	92.42	71.07	83.92	42.72	42.68	42.65	42.64	42.63
Apr	95.73	117.96	81.53	84.29	83.85	83.67	83.57	83.52
May	126.22	171.22	108.62	134.31	134.14	134.06	134.02	134.00
Jun	273.20	333.26	240.17	278.63	278.63	278.61	278.61	278.63
Jul	318.78	346.29	268.15	293.76	293.71	293.70	293.68	293.71
Aug	292.70	314.11	234.42	264.35	264.29	264.25	264.23	264.24
Sep	188.93	250.46	140.03	204.68	204.59	204.53	204.52	204.52
Oct	94.10	135.44	71.27	102.50	101.89	101.66	101.56	101.49
Nov	60.21	55.67	42.60	35.32	35.26	35.23	35.21	35.20
Dec	152.99	70.29	116.22	62.01	62.25	62.32	62.36	62.38
Annual	1966.01	1998.70	1590.18	1618.38	1617.49	1617.04	1616.80	1616.79

By observing the energy usage, it can be inferred that the energy consumption during winter months (Jan, Feb and Dec) marginally increases with increase in thermal conductivity. For the months (Mar, Apr, May, Sep, Oct and Nov), increase in k value decreases the energy consumption of the shed. And finally for the peak summer months (Jun, Jul and Aug), the energy consumption initially decreases with thermal conductivity and marginally increases at k value of 0.5 W/m-K.

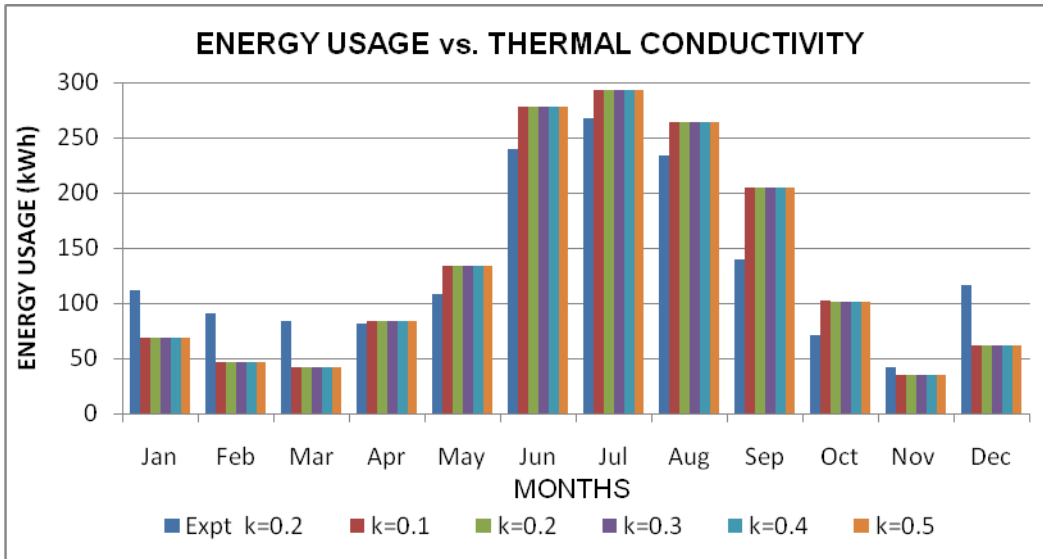


Figure 4.5 Variation of Thermal Conductivity of the PCM: Energy Usage

From Fig 4.5, it can be noticed that the experimental energy consumption at k value of 0.2 W/m-K is higher during winter months and lower during summer months. The differences in energy savings between various k values are also negligible as seen in the Table 4.12.

Table 4.12 Variation of Thermal Conductivity of the PCM: Energy Savings

Month	ENERGY SAVINGS (%)					
	Non PCM	With PCM				
	Expt	Energy+ k=0.1	Energy+ k=0.2	Energy+ k=0.3	Energy+ k=0.4	Energy+ k=0.5
Jan	28.82	8.73	8.41	8.30	8.25	8.21
Feb	19.54	18.28	18.01	17.92	17.88	17.86
Mar	9.20	39.89	39.95	39.98	40.01	40.02
Apr	14.83	28.54	28.92	29.07	29.15	29.20
May	13.94	21.56	21.66	21.70	21.73	21.74
Jun	12.09	16.39	16.39	16.40	16.40	16.39
Jul	15.88	15.17	15.18	15.19	15.19	15.18
Aug	19.91	15.84	15.86	15.87	15.88	15.88
Sep	25.88	18.28	18.31	18.34	18.34	18.34
Oct	24.26	24.32	24.77	24.94	25.02	25.06
Nov	29.25	36.55	36.66	36.71	36.74	36.76
Dec	24.03	11.78	11.45	11.33	11.28	11.25

Table 4.13 Variation of Thermal Conductivity of the PCM: Time Shift

Month	TIME SHIFT (min)					
	Expt	Energy+ k=0.1	Energy+ k=0.2	Energy+ k=0.3	Energy+ k=0.4	Energy+ k=0.5
Jan	0	0	0	0	0	0
Feb	0	0	0	0	0	0
Mar	0	0	0	0	0	0
Apr	0	0	3	3	3	3
May	0	0	0	0	0	0
Jun	60	0	0	0	0	0
Jul	15	0	0	0	0	0
Aug	45	0	0	0	0	0
Sep	30	0	0	0	0	0
Oct	0	0	9	9	9	9
Nov	0	0	0	0	0	0
Dec	0	0	0	0	0	0

There is no peak load shift by varying PCM thermal conductivity. Thus it can be concluded that the variation of the thermal conductivity of the PCM has no effect on the sheds as also evidenced by the annual energy consumption data.

#### 4.4.3 Variation of the Temperature Range of the PCM

The temperature range of the PCM in the walls, ceiling and floor were varied keeping all other parameters constant. The temperature ranges chosen for the simulation were: 21 to 25 °C, 23 to 27 °C, 25 to 29 °C, 27 to 31 °C, 29 to 33 °C and 31 to 35 °C. The temperature ranges were obtained by shifting the heat capacity values of 27 to 31 °C to the required ranges. The results obtained are presented below. From the Table 4.14, it is inferred that in winter season with increase in temperature range, the energy consumption faintly increases or remains fairly constant. For summer months, at low temperature ranges the

energy consumption is high and then decreases slightly with increasing temperature range and peaks up again at high temperature ranges. Time shift was observed significantly for all temperature ranges except for 27 to 31 °C with maximum observed for 23 to 27 °C followed by 21 to 25 °C.

Table 4.14 Variation of PCM Temperature Range: Energy Usage

Mon	Energy Usage (kWh)								
	Non PCM		With PCM						
	Expt	Energy y+	Expt	Energy+ 21 - 25 °C	Energy+ 23 - 27 °C	Energy+ 25 - 29 °C	Energy+ 27 - 31 °C	Energy+ 29 - 33 °C	Energy+ 31 - 35 °C
Jan	157.19	75.25	111.9	68.58	68.91	68.91	68.92	68.92	68.92
Feb	113.55	57.67	91.36	42.8	45.46	47.02	47.28	47.31	47.31
Mar	92.42	71.07	83.92	19.24	31.97	40.39	42.68	42.53	42.35
Apr	95.73	117.96	81.53	63.01	66.17	79.03	83.85	84.01	83.84
May	126.22	171.22	108.62	121.79	116.74	127.48	134.14	135.57	135.79
Jun	273.2	333.26	240.17	280.99	262.73	265.02	278.63	283.88	284.73
Jul	318.78	346.29	268.15	297.73	285.15	283.61	293.71	298.12	298.66
Aug	292.7	314.11	234.42	266.21	256.7	256.23	264.29	267.97	268.66
Sep	188.93	250.46	140.03	201.94	190.33	195.23	204.59	208.04	208.81
Oct	94.1	135.44	71.27	91.79	92.26	97.45	101.89	102.52	102.08
Nov	60.21	55.67	42.6	20.67	29.45	33.8	35.26	35.46	35.47
Dec	152.99	70.29	116.22	61	61.95	62.25	62.25	62.24	62.24
Ann	1966	1998.7	1590.18	1535.76	1507.82	1556.41	1617.49	1636.56	1638.87

The annual energy consumption decreases till the temperature range of 27 °C and then gradually increases. The least was observed for 23 to 27 °C while maximum consumption was observed for 31 to 35 °C. As seen in the Fig 4.6, the energy savings are low during the peak winter and summer months suggesting the fact that the PCM remains either mostly at solid phase (winter) or at liquid phase (summer). For the other months, the climate is favorable to maintain the PCM in the solid-liquid transition phase for a longer duration and hence it has more heat storage capability and energy savings.

Table 4.15 Variation of PCM Temperature Range: Energy Savings

Month	Energy Savings (%)						
	Non PCM	With PCM					
	Expt	Energy+ 21 - 25 °C	Energy+ 23 - 27 °C	Energy+ 25 - 29 °C	Energy+ 27 - 31 °C	Energy+ 29 - 33 °C	Energy+ 31 - 35 °C
Jan	28.82	8.87	8.43	8.42	8.41	8.41	8.41
Feb	19.54	25.78	21.18	18.48	18.01	17.97	17.97
Mar	9.20	72.93	55.01	43.18	39.95	40.16	40.41
Apr	14.83	46.58	43.91	33.00	28.92	28.78	28.93
May	13.94	28.87	31.82	25.55	21.66	20.83	20.69
Jun	12.09	15.69	21.16	20.48	16.39	14.82	14.56
Jul	15.88	14.02	17.66	18.10	15.18	13.91	13.75
Aug	19.91	15.25	18.28	18.43	15.86	14.69	14.47
Sep	25.88	19.37	24.01	22.05	18.31	16.94	16.63
Oct	24.26	32.23	31.88	28.05	24.77	24.31	24.63
Nov	29.25	62.87	47.09	39.29	36.66	36.31	36.29
Dec	24.03	13.21	11.87	11.44	11.45	11.45	11.45

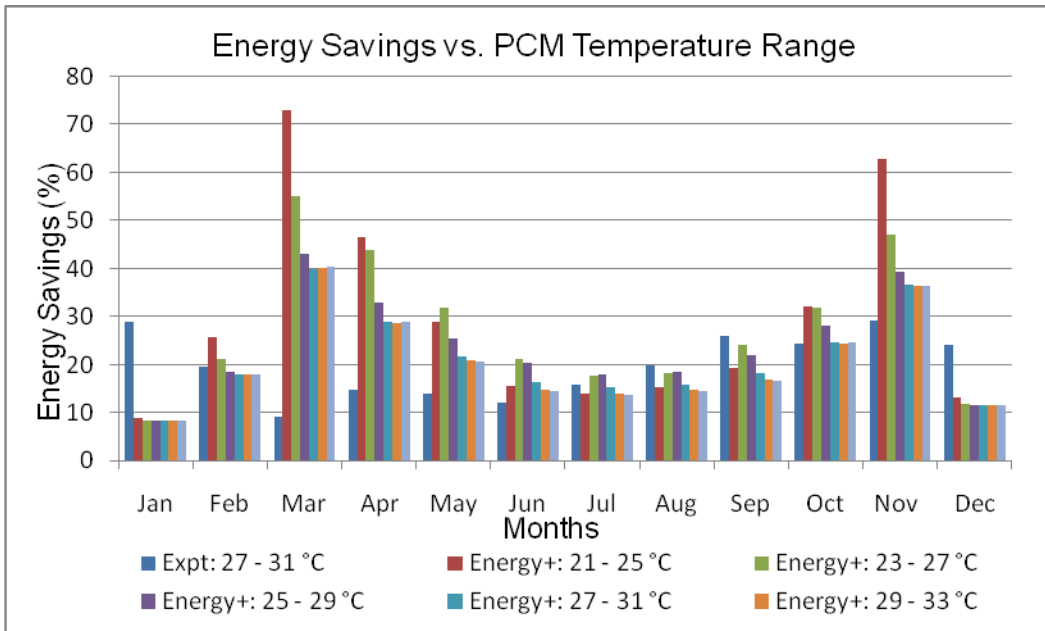


Figure 4.6 Variation of PCM Temperature Range: Energy Savings



Table 4.16 Variation of PCM Temperature Range: Time Shift

Month	Time Shift (min)						
	Expt 27 - 31 °C	Energy+ 21 - 25 °C	Energy+ 23 - 27 °C	Energy+ 25 - 29 °C	Energy+ 27 - 31 °C	Energy+ 29 - 33 °C	Energy+ 31 - 35 °C
Jan	0	0	0	0	0	0	0
Feb	0	0	0	0	0	0	0
Mar	0	0	0	0	0	0	0
Apr	0	42	96	15	3	6	15
May	0	33	63	6	0	3	3
Jun	60	12	33	24	0	12	18
Jul	15	15	30	21	0	21	21
Aug	45	12	57	45	0	0	12
Sep	30	18	72	30	0	3	9
Oct	0	33	51	9	9	9	9
Nov	0	0	0	0	0	0	0
Dec	0	0	0	0	0	0	0

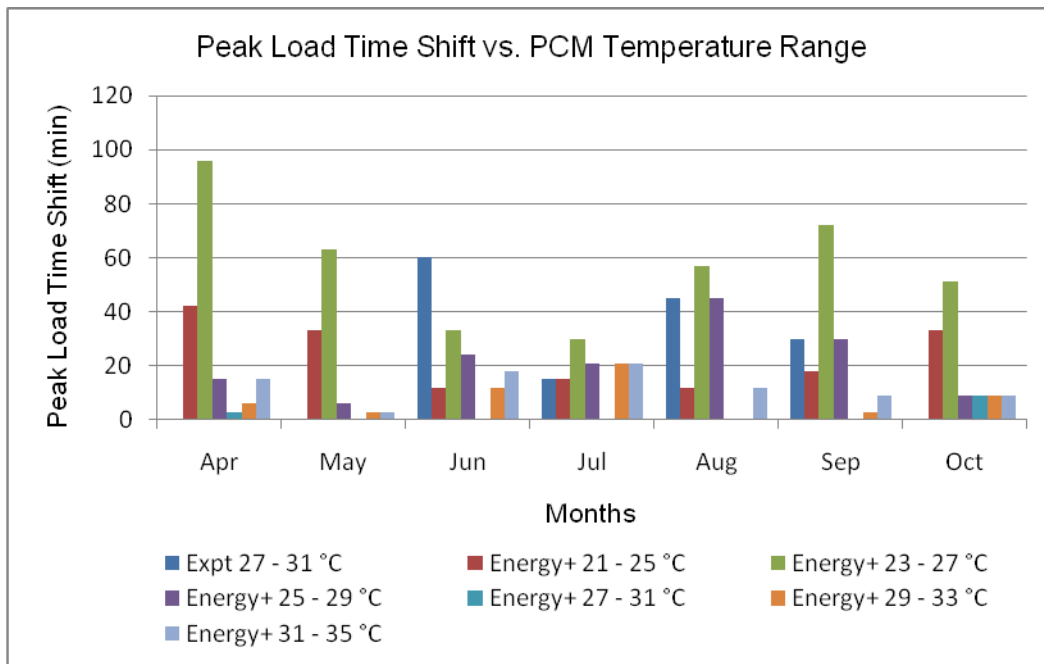


Figure 4.7 Variation of PCM Temperature Range: Peak Load Time Shift

As seen in the Fig 4.7, the peak load time shift is largest for the temperature range of 23 to 27 °C followed by 21 to 25 °C. The BioPCM was sandwiched

between the R13 and gypsum board for the walls. Hence most of the heat flow is reduced by the fiber glass insulation. The maximum temperature of the wall gypsum board ranged from 28.3 to 28.7 °C during the year for different walls. And the gypsum board temperature ranged between 23 to 27 °C for 40% of the year. The PCM being adjacent to the gypsum board would have had a slightly higher temperature considering the fact that it has a lesser thermal resistance.

The 23 to 27 °C PCM would have existed in this transition temperature range for a longer duration and would have stored more thermal energy than other temperature ranges. For instance, with a lower temperature range, the PCM would have melted completely and with a high temperature range, the PCM would have been in the solid state. Hence 23 to 27 °C have been favorable for light weight building constructions in Phoenix as it has the lowest annual energy consumption of all.

#### 4.4.4 Variation of Location of The PCM Layer

The PCM layer location was changed for two cases.

Case 1: PCM is located between T111 Siding and 2"x4" wood stud with R13 insulation for the walls and flanked between ceiling siding and 2"x6" wood stud with R19 insulation in the ceiling.

Case 2: PCM is located at two locations at either side of the insulation in the wall as well as ceiling cross-section. One between T111 Siding and 2"x4" wood studs with R13 insulation and another amid gypsum board and 2"x4" wood studs with R13 insulation for the walls. And between ceiling siding and 2"x6" wood studs with R19 insulation and sandwiched between gypsum board and 2"x6" wood studs with R19 insulation in the ceiling.

The PCM used in both cases had 27 – 31 °C temperature range. As seen in the Table 4.17 for the PCM shed with PCM located to the exterior of the envelope, the energy consumption remains fairly constant for Jan and Dec and increases marginally for the remaining months. This is due to the fact that the PCM melts quickly due to extreme environmental conditions (solar radiation and ambient temperature) allowing more heat to pass in during day time and in the night time most of the heat.

Table 4.17 Variation of PCM Location: Energy Usage

Month	Energy Usage (kWh)					
	Non PCM		With PCM			
	Expt	Energy+	Expt	Energy+ INT	Energy+ EXT	Energy+ EXT & INT
Jan	157.19	75.25	111.90	68.92	68.05	68.20
Feb	113.55	57.67	91.36	47.28	48.44	46.76
Mar	92.42	71.07	83.92	42.68	49.30	41.54
Apr	95.73	117.96	81.53	83.85	86.30	81.42
May	126.22	171.22	108.62	134.14	135.73	132.21
Jun	273.20	333.26	240.17	278.63	284.43	275.80
Jul	318.78	346.29	268.15	293.71	299.13	291.76
Aug	292.70	314.11	234.42	264.29	268.38	262.44
Sep	188.93	250.46	140.03	204.59	208.83	202.84
Oct	94.10	135.44	71.27	101.89	106.23	102.48
Nov	60.21	55.67	42.60	35.26	40.47	35.02
Dec	152.99	70.29	116.22	62.25	62.05	61.71
Annual	1966.01	1998.70	1590.18	1617.49	1657.34	1602.17

**Note:** INT refers that PCM is located close to the interior of the shed

EXT refers that PCM is located close to the outside environment

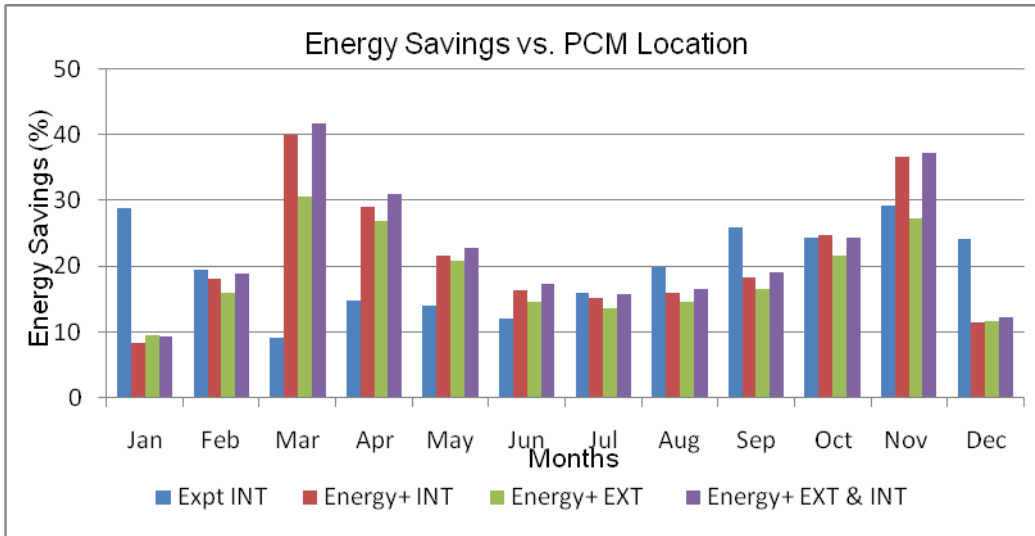


Figure 4.8 Variation of PCM Location: Energy Savings

released by the PCM goes to ambient than to the interior of the shed. The annual energy consumption is roughly 40 kWh more for the PCM located on the exterior. For the shed with PCM located on both on the interior and exterior, the energy usage slightly decreases and the annual consumption drops down by 15 kWh.

Table 4.18 Variation of PCM Location: Energy Savings and Time Shift

Month	ENERGY SAVINGS (%)				TIME SHIFT (min)			
	Non PCM	With PCM			Expt	Energy+ INT	Energy+ EXT	Energy + EXT & INT
	Expt	Energy+ INT	Energy+ EXT	Energy+ EXT & INT				
Jan	28.82	8.41	9.58	9.37	0	0	0	0
Feb	19.54	18.01	16.01	18.91	0	0	0	0
Mar	9.2	39.95	30.63	41.56	0	0	0	0
Apr	14.83	28.92	26.84	30.98	0	3	9	15
May	13.94	21.66	20.73	22.79	0	0	0	3
Jun	12.09	16.39	14.65	17.24	60	0	0	0
Jul	15.88	15.18	13.62	15.75	15	0	0	0
Aug	19.91	15.86	14.56	16.45	45	0	0	0
Sep	25.88	18.31	16.62	19.01	30	0	0	0
Oct	24.26	24.77	21.57	24.34	0	9	3	30
Nov	29.25	36.66	27.3	37.1	0	0	0	0
Dec	24.03	11.45	11.72	12.21	0	0	0	0

The load shift is marginally increased for PCM located at both the interior and the exterior. Hence it can be concluded that the location of the PCM doesn't contribute significant changes to the performance of the building. However, the suitable location would be close to the interior of the envelope with appropriate temperature range.

#### 4.4.5 Variation of Insulation Used in the Wall Cross-Section

In this study, the R-value of the wall cross-section was varied in both PCM and non PCM sheds with R11 and R19 and the results were compared with R13. The results obtained are shown in Table 4.19. It can be inferred that with increase in R value of the wall the energy consumption decreases as there is more resistance to heat flow. Significant reduction in energy consumption can be seen during the summer months. Adjusting the R value does not have any substantial effect on the energy savings and peak load time shift. However the annual energy consumption decreases with increasing insulation value.

Table 4.19 Variation of Insulation in the wall: Energy Usage

Month	Energy Usage (kWh)							
	Non PCM				With PCM			
	Expt R13	Energy+ R13	Energy+ R19	Energy+ R11	Expt R13	Energy+ R13	Energy+ R19	Energy+ R11
Jan	157.19	75.25	69.62	77.34	111.90	68.92	63.82	70.80
Feb	113.55	57.67	50.29	60.61	91.36	47.28	42.35	49.14
Mar	92.42	71.07	55.35	77.09	83.92	42.68	33.41	46.23
Apr	95.73	117.96	97.97	125.26	81.53	83.85	69.66	89.06
May	126.22	171.22	149.16	179.20	108.62	134.14	117.10	140.23
Jun	273.20	333.26	291.62	348.08	240.17	278.63	243.23	291.14
Jul	318.78	346.29	302.36	361.94	268.15	293.71	255.37	307.24
Aug	292.70	314.11	273.09	328.62	234.42	264.29	228.67	276.91
Sep	188.93	250.46	216.57	262.54	140.03	204.59	176.78	214.45
Oct	94.10	135.44	111.80	143.94	71.27	101.89	84.22	108.18
Nov	60.21	55.67	42.98	60.55	42.60	35.26	28.09	38.11
Dec	152.99	70.29	63.29	73.13	116.22	62.25	56.92	64.19
Annual	1966.01	1998.70	1724.10	2098.30	1590.18	1617.49	1399.62	1695.69

Table 4.20 Variation of Insulation in the Wall: Energy Savings and Time Shift

Month	Energy Savings (%)				Time Shift (min)			
	Non PCM	With PCM			Expt R13	Energy+ R13	Energy+ R19	Energy+ R11
	Expt R13	Energy+ R13	Energy+ R19	Energy+ R11				
Jan	28.82	8.41	8.33	8.46	0	0	0	0
Feb	19.54	18.01	15.80	18.93	0	0	0	0
Mar	9.20	39.95	39.64	40.03	0	0	0	0
Apr	14.83	28.92	28.90	28.90	0	3	0	3
May	13.94	21.66	21.49	21.74	0	0	0	0
Jun	12.09	16.39	16.59	16.36	60	0	0	0
Jul	15.88	15.18	15.54	15.11	15	0	0	0
Aug	19.91	15.86	16.27	15.73	45	0	0	0
Sep	25.88	18.31	18.37	18.31	30	0	3	0
Oct	24.26	24.77	24.66	24.84	0	9	6	0
Nov	29.25	36.66	34.65	37.05	0	0	0	0
Dec	24.03	11.45	10.05	12.23	0	0	0	0

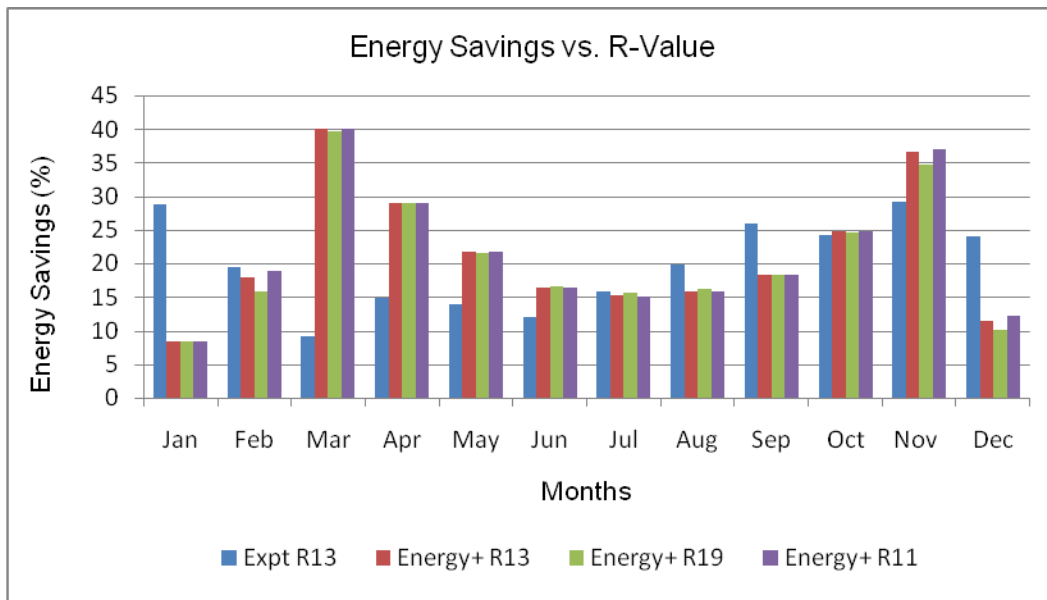


Figure 4.9 Variation of Insulation in the Wall: Energy Savings

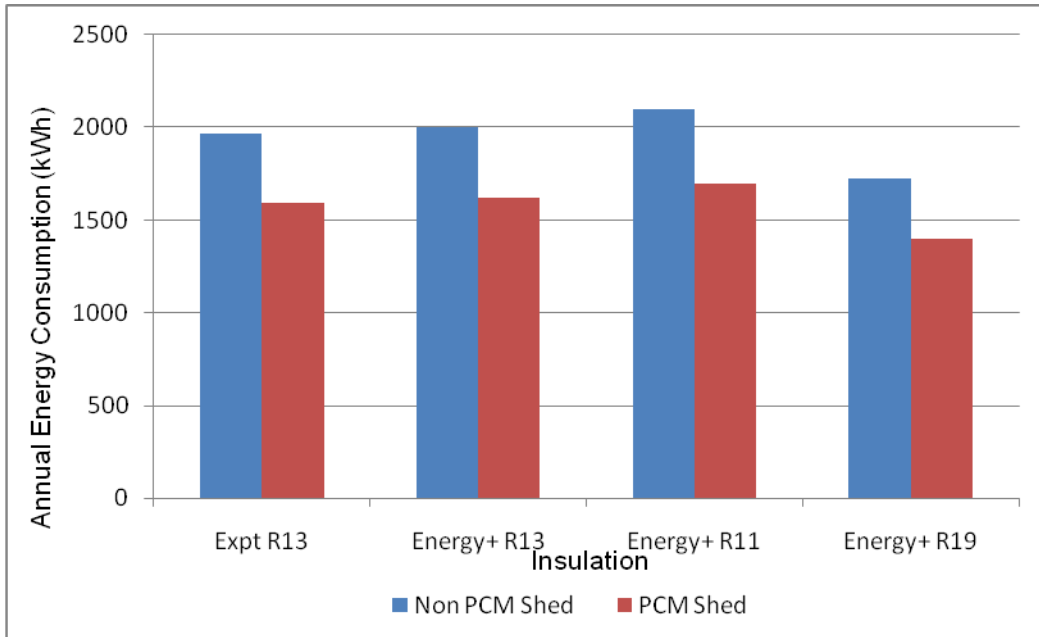


Figure 4.10 Variation of Insulation in the Wall: Annual Energy Consumption

#### 4.4.6 Variation of the PCM Temperature Range In The West and South Wall

The solar radiation is intense on the west and south side of the building. Hence in this analysis, a high PCM temperature range is used for the south wall, west wall, ceiling, floor and low temperature range used for north and east wall. The following two cases were simulated and results were compared with 27 to 31 °C, 25 to 29 °C and 23 to 27 °C in the building envelope:

Case 1: The south, west wall, ceiling and floor had PCM temperature range of 25 to 29 °C and the north and east wall had 23 to 27 °C PCM.

Case 2: The south, west wall, ceiling and floor had PCM temperature range of 27 to 31 °C and the north and east wall had 25 to 29 °C PCM.

Table 4.21 Combination of PCM: Energy Usage

Month	Energy Usage (kWh)							
	Non PCM		With PCM					
	Expt: 27 to 31 °C	Energy+: 27 to 31 °C	Expt: 27 to 31 °C	Energy+: 27 to 31 °C	Energy+: 25 to 29 °C	Energy+: 23 to 27 °C	Energy+ CASE 1	Energy+ CASE 2
Jan	157.19	75.25	111.90	68.92	68.91	68.91	68.92	68.92
Feb	113.55	57.67	91.36	47.28	47.02	45.46	46.96	47.28
Mar	92.42	71.07	83.92	42.68	40.39	31.97	38.91	42.53
Apr	95.73	117.96	81.53	83.85	79.03	66.17	75.96	83.05
May	126.22	171.22	108.62	134.14	127.48	116.74	124.45	132.19
Jun	273.20	333.26	240.17	278.63	265.02	262.73	264.76	273.02
Jul	318.78	346.29	268.15	293.71	283.61	285.15	283.80	288.97
Aug	292.70	314.11	234.42	264.29	256.23	256.70	255.01	260.77
Sep	188.93	250.46	140.03	204.59	195.23	190.33	191.91	201.38
Oct	94.10	135.44	71.27	101.89	97.45	92.26	95.07	101.06
Nov	60.21	55.67	42.60	35.26	33.80	29.45	33.19	35.15
Dec	152.99	70.29	116.22	62.25	62.25	61.95	62.26	62.24
Annual	1966.01	1998.70	1590.18	1617.49	1556.41	1507.82	1541.19	1596.57

Table 4.22 Combination of PCM: Energy Savings

Month	Energy Savings (%)					
	Non PCM	With PCM				
	Expt: 27 to 31 °C	Energy+: 27 to 31 °C	Energy+: 25 to 29 °C	Energy+: 23 to 27 °C	Energy+ CASE 1	Energy+ CASE 2
Jan	28.82	8.41	8.42	8.43	8.42	8.41
Feb	19.54	18.01	18.48	21.18	18.58	18.01
Mar	9.20	39.95	43.18	55.01	45.25	40.16
Apr	14.83	28.92	33.00	43.91	35.61	29.59
May	13.94	21.66	25.55	31.82	27.32	22.80
Jun	12.09	16.39	20.48	21.16	20.55	18.08
Jul	15.88	15.18	18.10	17.66	18.04	16.55
Aug	19.91	15.86	18.43	18.28	18.82	16.98
Sep	25.88	18.31	22.05	24.01	23.38	19.60
Oct	24.26	24.77	28.05	31.88	29.81	25.38
Nov	29.25	36.66	39.29	47.09	40.38	36.86
Dec	24.03	11.45	11.44	11.87	11.43	11.45



From Table 4.21, it can be noticed that the case one annual energy consumption is less than the shed with only 25 to 29 °C PCM in the building envelope. Similar lower energy usage can be seen for case two over 27 to 31 °C PCM. The potential advantage is to cut down cost by using lower temperature range or by reducing thickness of PCM on areas of the envelope where there are less external heat gain into the building.

Table 4.23 Combination of PCM: Time Shift

Month	Time Shift (min)					
	Expt: 27 to 31 °C	Energy+: 27 to 31 °C	Energy+: 25 to 29 °C	Energy+: 23 to 27 °C	Energy+ CASE 1	Energy+ CASE 2
Jan	0	0	0	0	0	0
Feb	0	0	0	0	0	0
Mar	0	0	0	0	0	0
Apr	0	3	15	96	39	15
May	0	0	6	63	36	3
Jun	60	0	24	33	36	0
Jul	15	0	21	30	21	21
Aug	45	0	45	57	45	0
Sep	30	0	30	72	51	9
Oct	0	9	9	51	48	27
Nov	0	0	0	0	0	0
Dec	0	0	0	0	0	0
Annual	150	12	150	402	276	75

Marginally increased savings could also be achieved by combination of PCM with different temperature ranges in the building envelope. Time shift (Table 4.23) has also increased significantly for case 1 PCM by just changing PCM temperature range in the east and south wall to 23 to 27 °C. Similarly for the case two, time shift has been observed for four months with more duration as

compared with the shed with only 27 to 31 °C. Hence the idea of having higher PCM temperature range on west wall, south wall and ceiling would help to achieve peak load shift, energy and cost savings.

#### 4.4.7 Variation of the PCM thickness

The thickness of the BioPCM in the wall cross-section was 0.002 m and in the floor/ceiling it was 0.01 m. The thickness for the continuous layer of the PCM was calculated after considering the same volume of PCM used for experimental testing.

4.24 Variation of the BioPCM Thickness

Energy Saving (%)					Time Shift (min)				
Expt	Energy+ T	Energy+ 2T	Energy+ 3T	Energy+ 4T	Expt	Energy+ T	Energy+ 2T	Energy+ 3T	Energy+ 4T
28.82	8.41	9.00	9.56	10.08	0	0	0	0	0
19.54	18.01	20.65	22.36	23.45	0	0	0	0	0
9.20	39.95	47.64	52.25	55.02	0	0	0	0	0
14.83	28.92	33.17	35.74	37.39	0	3	15	15	0
13.94	21.66	23.59	24.64	25.37	0	0	3	0	0
12.09	16.39	17.33	17.96	18.54	60	0	0	0	0
15.88	15.18	15.85	16.19	16.52	15	0	0	0	0
19.91	15.86	16.47	16.76	16.98	45	0	0	0	0
25.88	18.31	19.44	20.10	20.54	30	0	12	0	0
24.26	24.77	26.45	26.94	27.03	0	9	9	3	0
29.25	36.66	42.76	46.20	47.74	0	0	0	0	0
24.03	11.45	12.43	13.18	13.82	0	0	0	0	0

In the table 4.24, T refers to original thickness, 2T refers to two times the original thickness, 3T refers to three times the original thickness and 4T refers to four times the original thickness. The amount of BioPCM that can be used is only limited by the cost and the wall thickness. More PCM means that there is more time during the solid-liquid transition phase, hence more thermal energy is being stored. Hence we have more savings with increasing thickness as seen in the

table 4.24. The time shift reduces with increasing thickness and no concrete reason is available for this.

#### 4.5 Virgin and Experimented PCM



Figure 4.11 Virgin (left) and Experiment (right) BioPCM

Figure 4.11 shows the virgin BioPCM and the experimented BioPCM after the testing period. The encapsulation of the virgin PCM is more intact and maintains a good square shape. On the other hand, the experimented PCM which had undergone hundreds of melting and solidification cycles has lost its shape and has deformation severely. The mass of the virgin and used PCM are respectively 0.42 kg (0.925 lb) and 0.21 kg (0.462 lb) for a mat size of 1.5" x 9.75"). Hence, the used PCM has a mass reduction of 50%. One possible theory is the loss of moisture from the PCM through the plastic container leading to a decrease in the volume, causing the abnormal shape. The instance at which this volume loss occurred is unknown. This is only a speculation and more experimental studies have to be carried out to clearly understand the cause of this deformation. Hence future research work will involve finding a more suitable encapsulation material for the BioPCM.

## Chapter 5

### CONCLUSION AND FUTURE WORK

#### 5.1 Summary and Conclusion of Present Work

In this research, experimental evaluation of organic-based BioPCM in the building envelope is discussed and compared with traditional building construction without it. The setup was tested for climatic conditions of Phoenix, Arizona. EnergyPlus was also used to validate the experimental results and other parametric studies to optimize PCM performance were carried out.

The key conclusions in the experimental setup are:

- The maximum and minimum energy savings during summer was observed for September (25.9 %) and June (12.1 %) respectively.
- The maximum and minimum energy savings during winter was observed for November (29.3 %) and March (9.2 %) respectively.
- The peak load time shift was highest for the month of June with 60 min and least for the month of July with 15 min.
- The residential cost savings was highest for the month of January (31.3 %) and least for the month of March (9.6 %).
- Similarly, the business cost savings was highest for the month of November (28.2 %) and least for the month of March (10.5 %).
- The energy reduction during on-peak hours was maximum during June (9.5 %) and minimum occurred during September (4.2 %)

The key conclusions of the simulation are:

- In comparison with the experimental results, the simulation energy consumption values are half during winter and slightly greater for the summer months. The reason might be due to continuous layer of PCM used in the simulation which allows greater heat gain into the building.
- The time shift was observed for a very short span only for the months of April (3 min) and October (9 min).
- The variation of thermal conductivity had no effect on the performance of the building with respect to energy savings or peak load time shift.
- The PCM temperature variation yielded good results for the range of 23 to 27 °C with huge energy savings and maximum peak load time shift. Hence this temperature range is ideal for light construction buildings in Phoenix.
- The variation of PCM location from the interior to the exterior of the envelope had no significant effect on the building performance.
- Insulation value of R19 in the walls reduced the energy consumption from 1618 kWh (R13) down to 1400 kWh at the expense of increased cost. However there was no peak load time shift.
- By having a low temperature range of PCM on the south and west wall, the energy consumption decreased by 20 kWh annually. But, there was significant increase in the time shift for about 6 months from the start to the end of summer seasons

## 5.2 Future Work

Some of the potential works with PCM that can be pursued are:

- Modeling a realistic PCM layer with discrete block with air gaps in between.
- Exploring performance of PCM with medium and heavy construction materials.
- Investigating the behaviour of PCM with different locations and finding a suitable operating temperature range for different cities.
- Evaluating the usage of PCM in buildings in the colder climate regions.
- Finding a better encapsulation material to hold the PCM as it can lose the moisture content by its repetitive cyclic usage.

## REFERENCES

Herald Mehling and Luisa F Cabeza, "Heat and Cold Storage with PCM, An up to date introduction into basics and application" Springer, 2008

Ival O. Salyer and Anil K.Sircar, "A Review of Phase Change Materials Research for Thermal Energy Storage in Heating and Cooling Applications at the University of Dayton from 1982 to 1996", International Journal of Global Energy Issues, Vol 9, No 3, 1997, pgs 183-198.

Fatih Demirbas, "Thermal Energy Storage and Phase Change Materials: An Overview", Energy Sources, Part B, 1:85-95, 2006

Ibrahim Dincer, Marc A.Rosen, "Thermal Energy Storage Systems and Applications" Wiley Publication.

B.Frank, "Using Phase Change Materials (PCMs) for Space Heating and Cooling in Buildings", Proceedings of 2004 AIRAH Performance Enhanced Buildings Environmentally Sustainable Design Conference.

A.Pasupathy, R.V.Seeniraj, "Experimental Investigation and Numerical Simulation Analysis on the Thermal Performance of a Building Roof Incorporating Phase Change Material (PCM) for Thermal Management", Applied Thermal Engineering, 2008, pgs 556-565.

Chao Chen, Haifeng Guo, "A New Kind of Phase Change Material (PCM) for Energy-Storing Wallboard", Energy and Buildings 40(2008), pgs 882-890.

M.J.Huang, P.C.Eames, "The Application of a Validated Numerical Model to Predict the Energy Conservation Potential of Using Phase Change Materials in the Fabric of a Building", Solar Energy Materials & Solar Cells 90 (2006), 1951-1960.

K.Nagano, S.Takeda, T.Mochida, K.Shimakura, T.Nakdamura, "Study of a Floor Supply Air Conditioning System using Granular Phase Change Material to Augment Building Mass Thermal Storage – Heat Response in Small Scale Experiment", Energy and Buildings, Vol 36, pgs 436 – 446.

Farid MM, Chen XD. "Domestic Electric Space Heating with Heat Storage". Proc Instn Mech Engrs 1999;213: pgs 83–92

"Using Phase Change Material (PCMs) For Space Heating and Cooling in Buildings", 2004 AIRAH performance enhanced buildings environmentally sustainable design conference.

S.L.Chen, "One-Dimensional Analysis of Energy Storage in Packed Capsules", Journal of Solar Energy Engineering, May 1992, Vol 114, pgs 127-130.

H. Mehling, S.Hiebler, "Review of PCM in Buildings" current R&D. Paper presented at the IEA Annex 17 Workshop in Arvika (Sweden) held in 8th June, 2004.

<http://www.nrel.gov/midc/apps/daily.pl?site=PFCI&start=20060201&yr=2009&mo=11&dy=11>

<http://www.amana-ptac.com/Home/Products/WRAC/HeatPumpAH09/tabid/544/Default.aspx>

<http://www.tainstruments.com/product.aspx?id=15&n=1&siteid=11>

<http://www.solidsolar.com>



